Geoengineering and Seismological Aspects of the Iwate Miyagi-Nairiku, Japan Earthquake of June 14, 2008

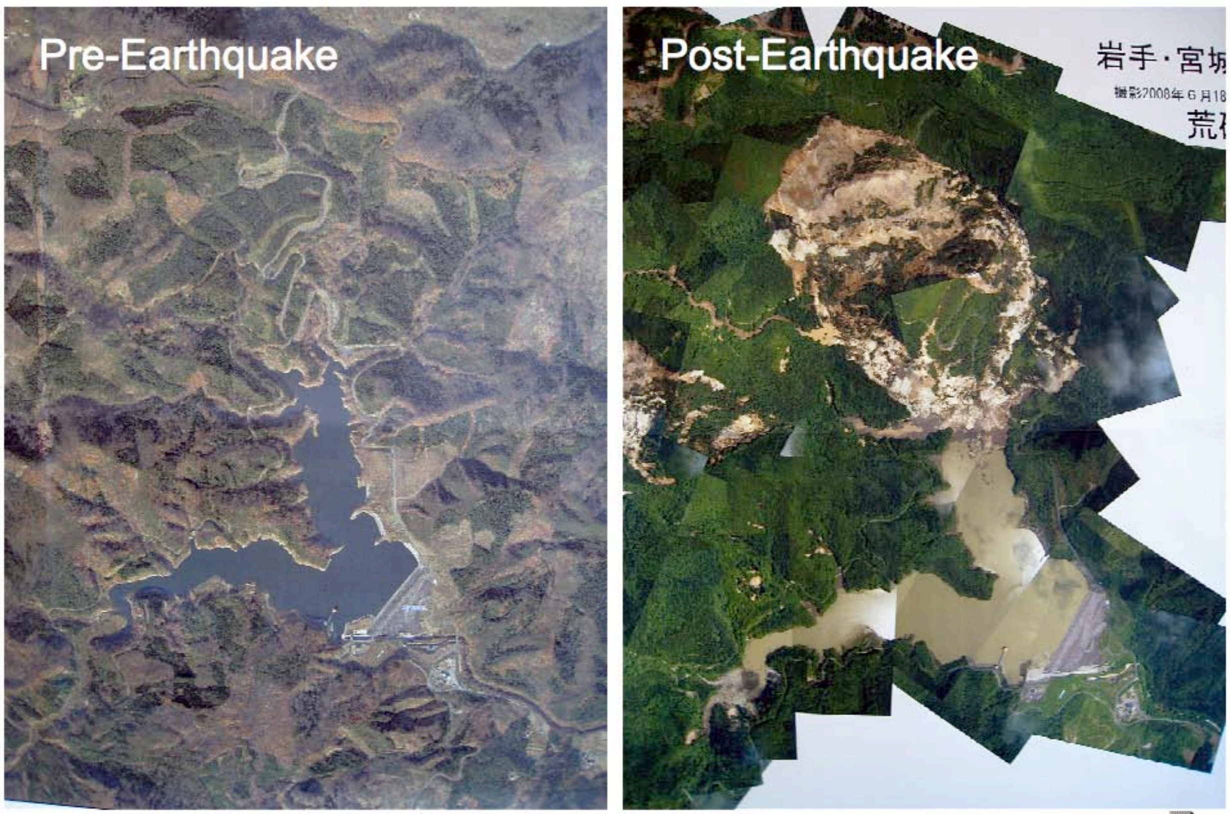

Robert Kayen, Brady Cox, Jorgen Johansson, Clint Steele, Paul Somerville, Kazuo Konagai, Yu Zhao, Hajime Tanaka

GEER Web Report 2008 v.1

September 12, 2008

Contents

Geoengineering and Seismological Aspects of the Iwate Miyagi-Nairiku, Japan Earthquake of June 14, 2008

Robert Kayen[1], Brady Cox[2], Jorgen Johansson[3], Clint Steele[1], Paul Somerville[4], Kazuo Kongai[3], Yu Zhao[3], Hajime Tanaka[3]

GEER Report 2008.2 v.1

September 12, 2008

Section 1: Introduction

The Iwate Miyagi-Nairiku earthquake occurred in an interior and rural mountainous region of Tohoku, Japan in steep terrain (refer to Figure 1.1). Geoengineering damage was almost entirely confined within a 35-km radius of the epicenter. Landslide impacts to transportation infrastructure and moderate deformations of earth dams provide some of the most important geoengineering case histories for the Iwate Miyagi-Nairiku earthquake. Remarkably, there were no observations of liquefaction from this event. The Iwate Miyagi-Nairiku earthquake follows several other damaging earthquakes in the Tohoku region of Japan in the last four years, though it was substantially less damaging than either the Niigata Chuetsu earthquake of 2004 that devastated the Nagaoka region of Niigata; or the Niigata Chuetsu-Oki earthquake of 2007 in the coastal area of Kashiwazaki City and Kariwa town of southwestern Niigata Prefecture.

American Plate in northern Japan, where the Pacific plate is moving west-northwest with respect to North America at a rate of approximately 8.3 cm/yr. The hypocenter of the earthquake indicates shallow thrusting motion in the upper (Okhotsk) plate, above the subducting Pacific plate, which lies at approximately 80 km depth at this location.
http://earthquake.usgs.gov/eqcenter/eqarchives/significant/sig_2008.php

[1] United States Geological Survey; 345 Middlefield Road, MS999; Menlo Park,CA
[2] University of Arkansas, Department of Civil Engineering, BELL 4190, Fayetteville, AR 72701
[3] Tokyo University, 4-6-1 Komaba Meguro-Ku, Tokyo 153-8505, Japan
[4] URS Corporation, 566 El Dorado Street, Pasadena, CA 91101-2560

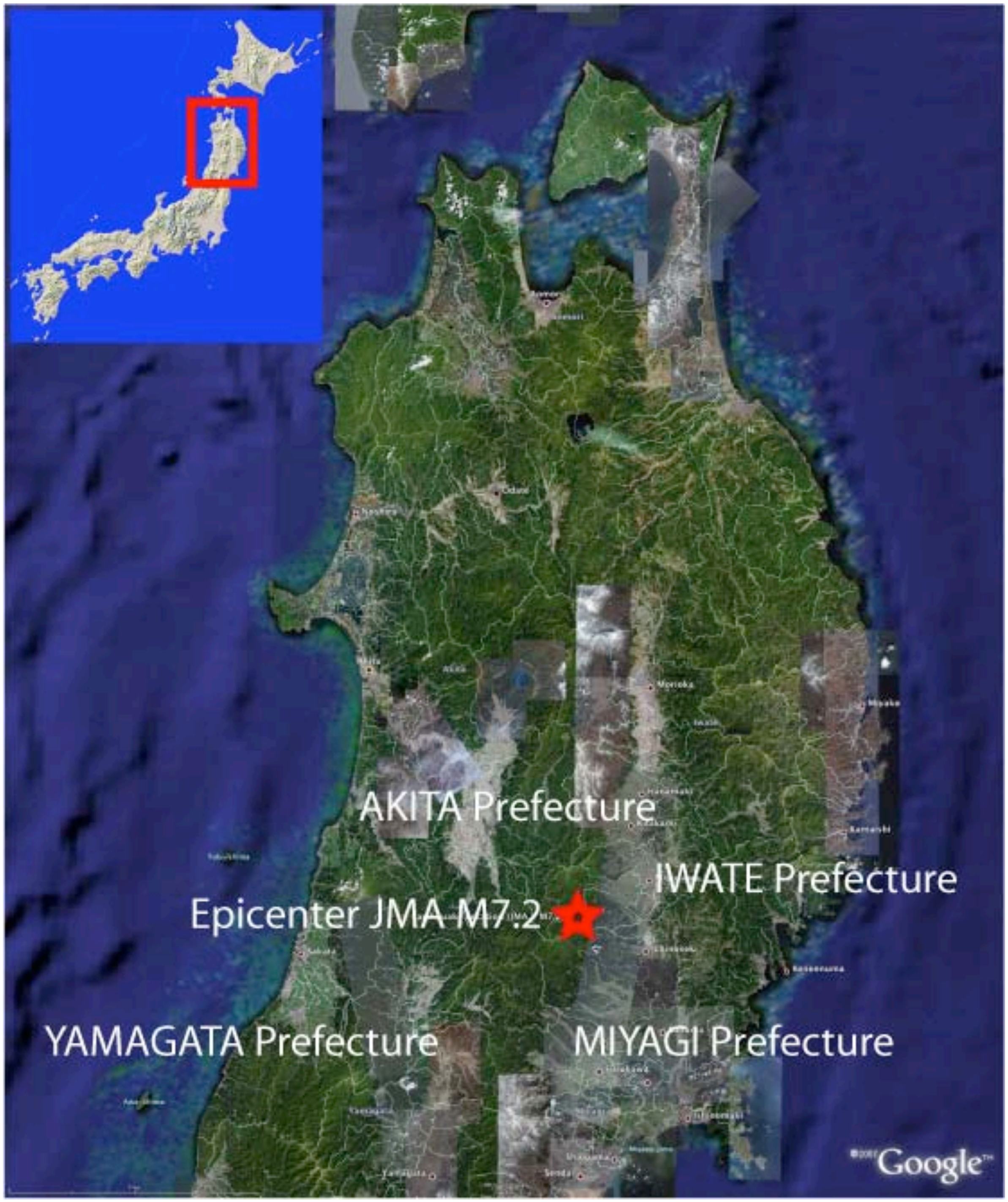

Figure 1.1 Location map of Tohoku region of Japan, the epicenter of the event, and the four effected prefectures of Akita, Iwate, Miyagi, and Yamagata.

The Mw 6.9 Honshu earthquake of June 13th 2008 (UTC; June 14, 2008 local time) occurred in a region of convergence between the Pacific Plate and the Okhotsk section of the North

The earthquake was recorded on many strong motion instruments, including the K-Net and Kik-Net stations of the National Research Institute for Earth Science and Disaster Prevention (NIED). A very large peak acceleration of nearly 4g was recorded on the ground surface at station IWTH25, located near the epicenter of the earthquake. The strongest shaking was measured in the cities of ŌsShū (Iwate) and Kurihara (Miyagi), both at the 6 Upper level of the JMA seismic intensity scale. Over 200 felt aftershocks were recorded in the first 24 hours, with about 400 total in the first seven days.

The 2008 Iwate Miyagi-Nairiku earthquake was accompanied by several surface fault related features along a 20-km long NNE-SSW stretch from Ikawa district in the North to Aratozawa Dam in the South. Surface fault related features were observed at over 10 locations, but resulted in very little structural damage due to the sparsely populated region. Near Aratozawa Dam (Site 27), a strike slip fault trace was discovered very close to the head scarp of an enormous landslide. How this fault is related to triggering the large landslide needs to be clarified. Landslides caused by the earthquake were primarily deep-seated rotational slides in weathered bedrock; collapses of corner buttresses composed of both rock or weathered rock and soil; rockfall and rock avalanches; shallow translational slides and shallow debris flows. Shallow landslides were common at road cuts in mountain terrain. One particularly enormous event was the previously mentioned landslide near Aratozawa Dam. The total volume of the landslide was estimated to be 50 million cubic meters, of which approximately 1.5 million cubic meters slid into the reservoir causing a wave that overtopped the spillway. The massive landslide above Aratozawa Dam, resulted in a spectacular roadway failure where the landslide carried a 3.5 km-long section of road downslope. Numerous other large landslides occurred and were largely within a 15-km radius around the earthquake epicenter effecting reservoirs. Landslides severed transportation arteries between southern Akita, Iwate, and Miyagi prefectures. Near the epicenter, a number of large landslides completely swept away portions of roads (Site 31), and in one instance caused the complete collapse of a large steel frame bridge (Site 36). Roadway damage throughout the epicentral region was ubiquitous. In some instances, landslide or rock fall debris covered the roadway blocking passage, while in other cases landslides completely carried roads downhill. Embankment failures ranged from small cracks in the asphalt to large vertical and horizontal offsets.

Several earthen dams suffered moderate deformations due to settlement of the crest, and these provide excellent case histories. At one dam, the Isawa Dam, one worker was killed by rockfall at the dam abutment.

Reconnaissance Method

A reconnaissance team sponsored by the Geo-Engineering Earthquake Reconnaissance (GEER) activity of the NSF was organized and sent to the epicentral region 10 days after the earthquake to assess the geo-engineering and soil-related structural damage aspects of the earthquake. The field reconnaissance team members were Robert Kayen (team leader; USGS), Brady Cox (University of Arkansas), Jorgen Johansen, Yu Zhao and Hajime Tanaka (University of Tokyo). The GEER team's main goal was to quantify the spatial extent and magnitude of ground failures, soil liquefaction, landslides, and damage to bridges, piers, ports, harbors, lifeline systems, and critical structures.

During the five-day reconnaissance, from June 26 through June 30, two vehicles were used to traverse most of the roads of the epicentral region. Each vehicle had a team equipped with handheld two-way radios, digital cameras, maps, computers for recording site logs, and GPS units for recording track logs and site locations. In the evening, the reconnaissance team met to merge the GPS data, site logs, and digital photos into a common database. In the field, a Google Earth KML markup language file was generated to display all the written observations on dynamic digital maps (Figure 1.2) and damage-specific maps (see http://walrus.wr.usgs.gov/infobank/t/toh08jp/html/t-oh-08-jp.meta.html). By observing damage in the Google Earth program, the team identified unexplored areas for the next day's reconnaissance, spatial trends in the observations, and any errors in the GPS logs and typed observations. The .kml files also allow GEER members to take virtual tours of the damage zone and plan for additional investigations.

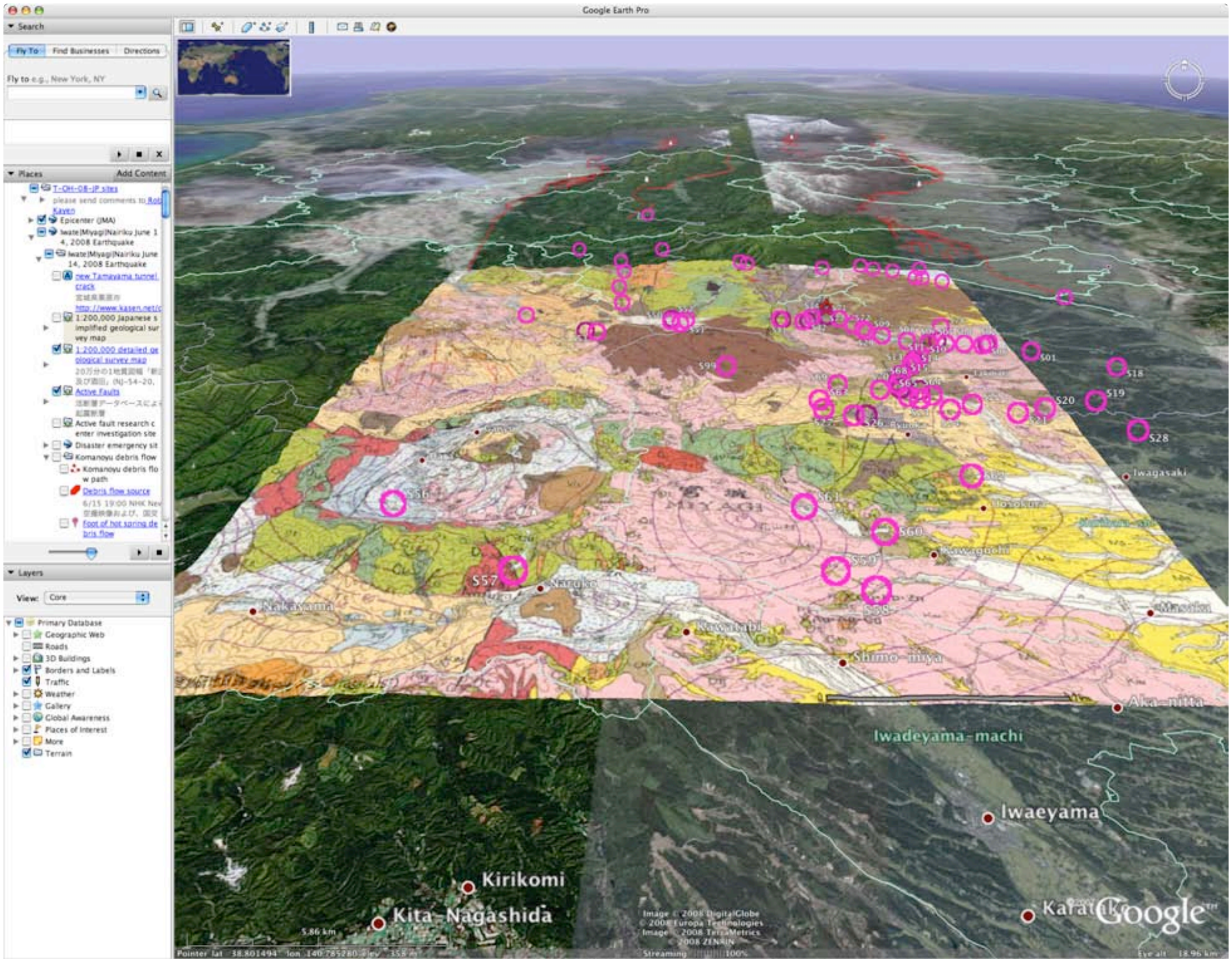

Figure 1.2. An interactive observation map file of the Iwate MiyagiNairiku Earthquake of June 14, 2008 can be downloaded at http://walrus.wr.usgs.gov/infobank/t/toh08jp/html/t-oh-08-jp.meta.html . The map has GEER reconnaissance sites, geologic maps, location of known mapped faults prior to the earthquake, and the event epicenter.

The authors of this report recommend downloading and opening the .kmz Google Earth map file to navigate through the report observation sites as they are described in the text. Click-ing on the individual site name in the waypoints folder will direct the program to fly to that site. The t-oh-08-jp-2.sites.kmz file will be updated regularly on the USGS server. When the reader revisits the data set, remove any older versions of the .kmz file from Google Earth and then go to the URL http://walrus.wr.usgs.gov/infobank/t/toh08jp/html/t-oh-08-jp.sites.kmz and download the latest file.

High-resolution topographic data sets of the most significant damage to earth dams and tunnels were collected to preserve the event by using the USGS terrestrial Light Detection and Ranging (LiDAR) system. Terrestrial LiDAR data were collected at Aratozawa Dam (Site 27, N 38.8837°, 140.8560°), Masazawa Dam (Site 42, N 39.100905°, E140.966859), and Shintamayama Tunnel (Site 64, N 38.9009°, E140.924°). The terrestrial LiDAR data collection technique consists of sending and receiving laser pulses to build a point file of 3-D coordinates of virtually any reflective surface. The time of travel for a single pulse reflection is measured along a known trajectory in such a way that the distance from the laser and consequently the location of a point of interest is computed. The USGS system consisted of a Riegl Z420 instrument mounted on a tripod platform and a photogrammetric overlay system using a calibrated digital camera. The instrument captured data at approximately 12,000 points per second, with a typical range of several hundred meters and at an accuracy of 15 mm for each point. Global georeferencing was performed at the Aratozawa dam site with the assistance of a total station used to site on LIDAR reflectors. At the Masazawa Dam and inside the Shintamayama Tunnel, a local project coordinate system was developed by placing non-georeferenced LIDAR reflectors in the field of view of the project scans. Data from these sites will be made available in digital format once they are processed.

This reconnaissance report is organized into sections that describe geotechnical and structural aspects of the earthquake damage. Section 2 describes seismological aspects, Section 3 describes surface rupture features, Section 4 describes landslides, Section 5describes damage to transportation systems, Section 6 describes damage to earth dam structures, Section 7 describes SASW measurements at Aratozawa Dam.

USGS, 2008, http://earthquake.usgs.gov/eqcenter/recenteqsww/Quakes/us2008tfdp.php#details

JMA (2008) http://www.jma.go.jp/jma/press/0806/14d/h20iwate-miyagi-4.html

Section 2 – Seismological Aspects

The 2008 Iwate earthquake of June 14, 2008 struck the mid Tohoku region, northeastern Honshū, Japan. The Japan Meteorological Agency (JMA) officially named this earthquake the Iwate-Miyagi Nairiku Earthquake of 2008. This earthquake occurred in the southwestern Iwate Prefecture at 8:43 JST on Saturday morning, June 14 (23:43 UTC on June 13). The JMA magnitude was estimated at M_j 7.2, and the moment magnitude measured by the USGS was M_w 6.9. The epicenter was located at 39°01.7′N, 140°52.8′E, about 85 kilometers (55 mi) north of Sendai and about 385 kilometers north-northeast of Tokyohttp://en.wikipedia.org/wiki/2008_Iwate-Miyagi_Nairiku_earthquake - cite_note-5#cite_note-5.

The strongest shaking was measured in the cities of Ōshū (Iwate) and Kurihara (Miyagi), both at the 6 Upper level of the JMA seismic intensity scale. Over 200 felt aftershocks were observed in the first 24 hours, with about 400 total in the first seven days. The largest ones (with M_j 5.0 or greater) were: (1) June 14, 9:20, M_j 5.7, maximum seismic intensity of 5 Lower; (2) June 14, 12:27, M_j 5.2, maximum seismic intensity of 4; and (3) June 16, 23:14, M_j 5.3, maximum seismic intensity of 4. Between June 21 and July 1, four to 12 felt aftershocks were observed each day, with maximum seismic intensities of 3.

The earthquake occurred in a region of convergence between the Pacific Plate and the Okhotsk section of the North American Plate in northern Japan, where the Pacific plate is moving west-northwest with respect to the North American plate at a rate of approximately 8.3 cm/yr. The hypocenter of the earthquake indicates shallow thrusting motion in the upper (Okhotsk) plate, above the subducting Pacific plate, which lies at approximately 80 km depth at this location.

A rupture model of the earthquake was developed by Hikima (2008) immediately following the earthquake. The finite fault model indicates a fault plane dipping at a shallow angle to the west and this was assumed to be the fault rupture plane. The inferred amount of slip on the fault plane is shown in Figure 2.1.

The earthquake was recorded on many strong motion instruments, including the K-Net and Kik-Net stations of the National Research Institute for Earth Science and Disaster Prevention **(**NIED**)**. Maps of recorded peak acceleration and peak velocity are shown in Figures 2.2 and 2.3. A comparison of the recorded peak acceleration and peak velocity with the empirical ground motion model of Si and Midorikawa (1999) for shallow crustal earthquakes is shown in Figure 2.4. There is close agreement between the recorded ground motions and the model.

A very large peak acceleration of nearly 4g was recorded on the ground surface at station IWTH25, located near the epicenter of the earthquake. The recorded acceleration and velocity time histories recorded at this station at a depth of 260 meters below the surface (top) and at the ground surface (bottom) are shown in Figure 2.5. The downhole recording does not have exceptionally large peak acceleration, indicating that the large ground motion recorded at the surface was probably caused by a local amplification effect in the intervening 260 meters. The amplification effect was much larger for peak acceleration than for peak velocity.

References

Hikima, K. (2008). 2008 Iwate-Miyagi Nairiku Earthquake Preliminary Finite Fault Model. http://www.eri.u-tokyo.ac.jp/topics/Iwate2008/source_eng.html. Last updated June 16, 2008.

Si, H. and S. Midorikawa, 1999, Attenuation Relations for Peak Ground Acceleration and Velocity Considering Effects of Fault Type and Site Condition, Journal of Struct. Construct. Eng. (Transactions of AIJ), No. 523, 63-70 (in Japanese).

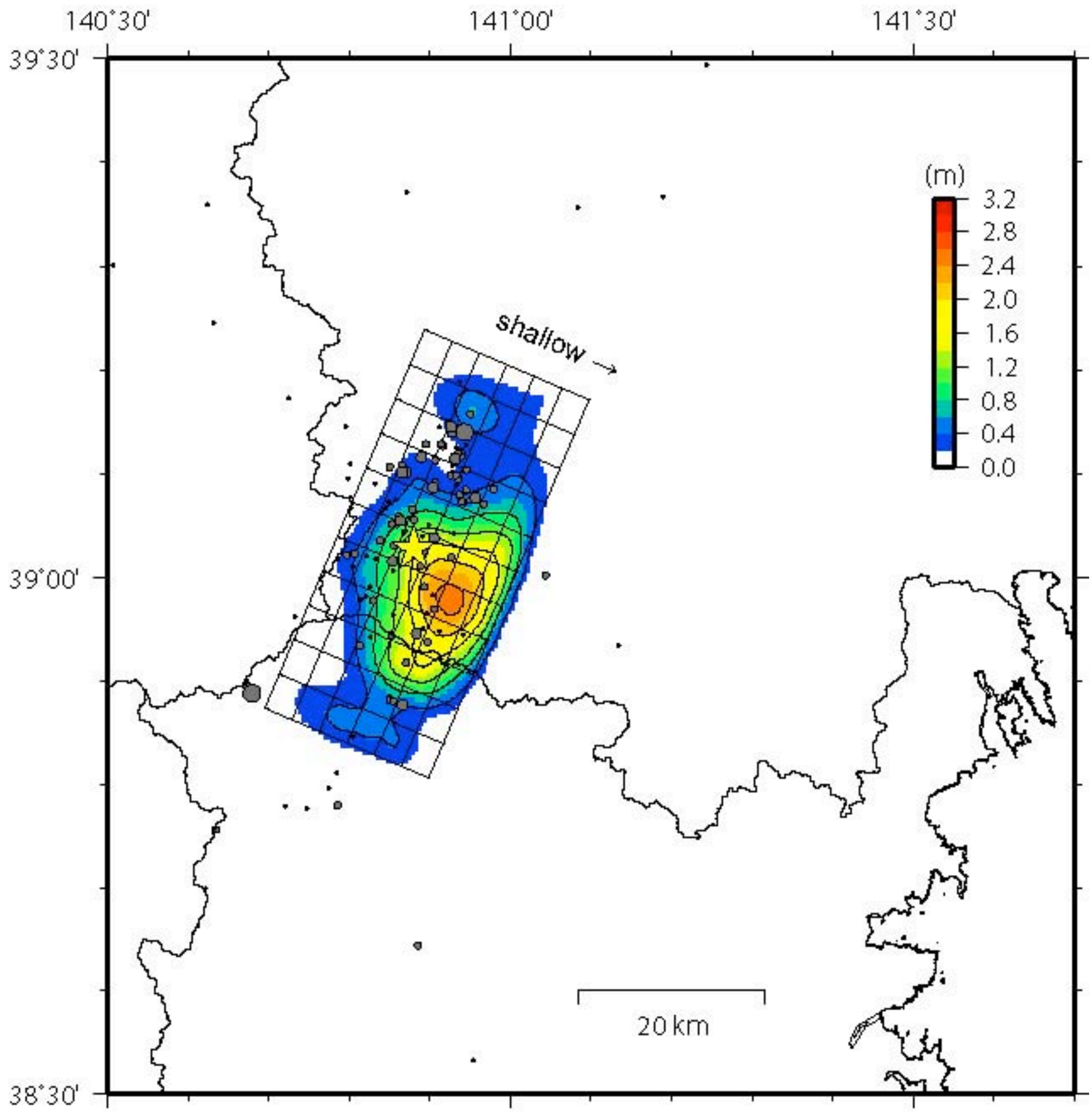

Figure 2.1. Slip model of the earthquake, with slip in the meters shown both in contours and color coding. Source: Hikima (2008).

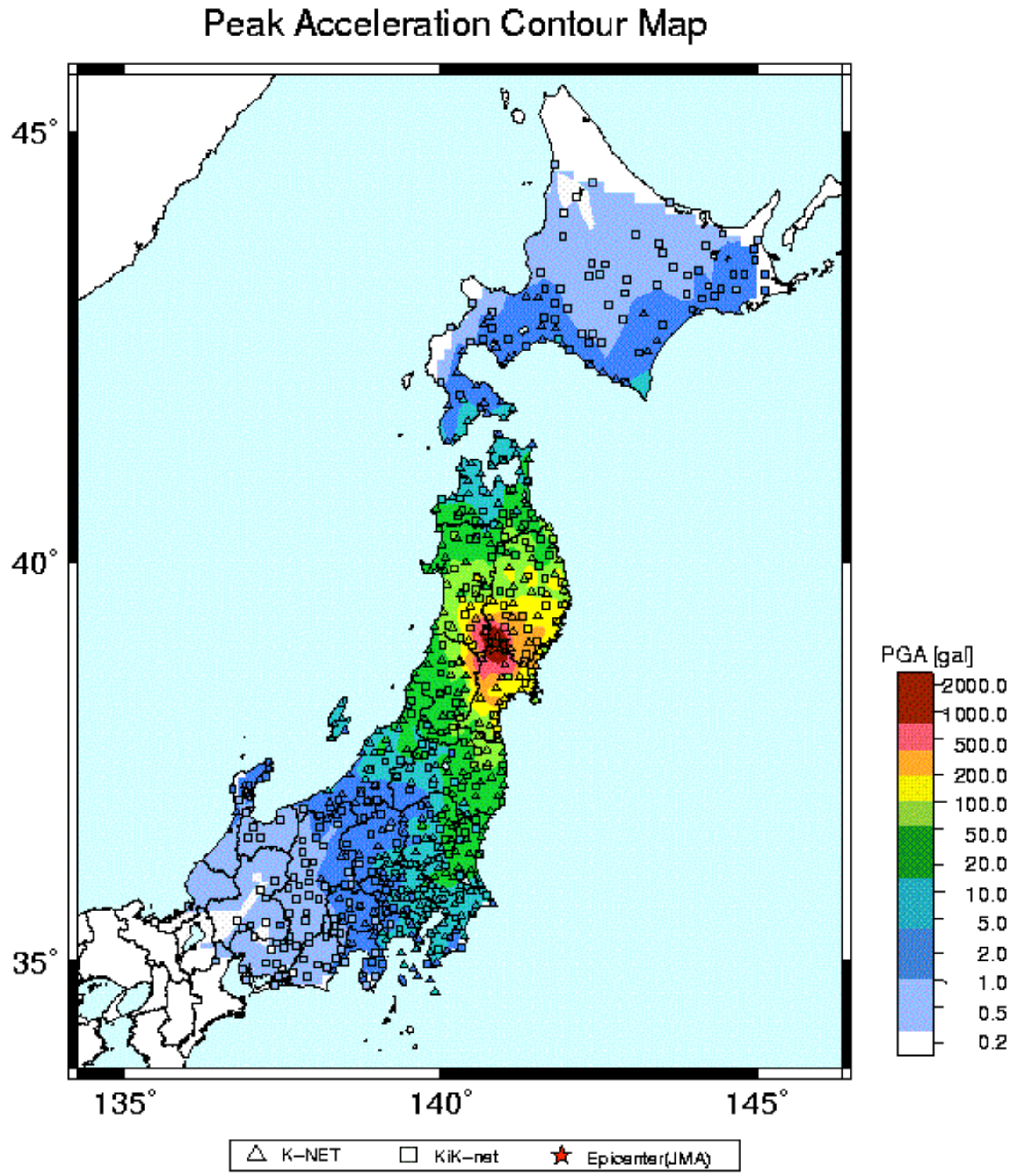

K-NET NIED

KiK NIED

Figure 2.2. Map of recorded peak horizontal acceleration. Source: NIED (2008).

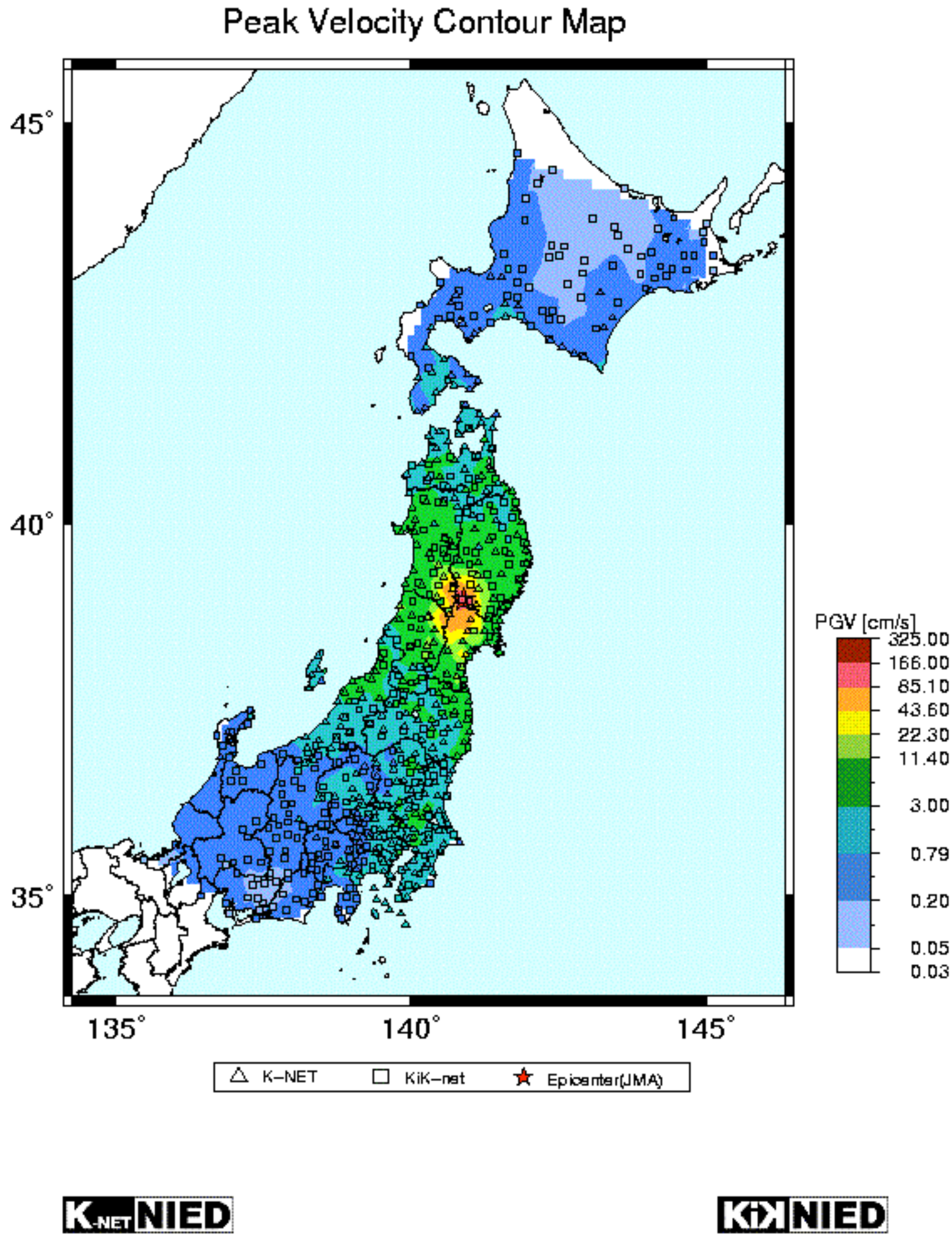

Figure 2.3. Map of recorded peak horizontal velocity. Source: NIED (2008).

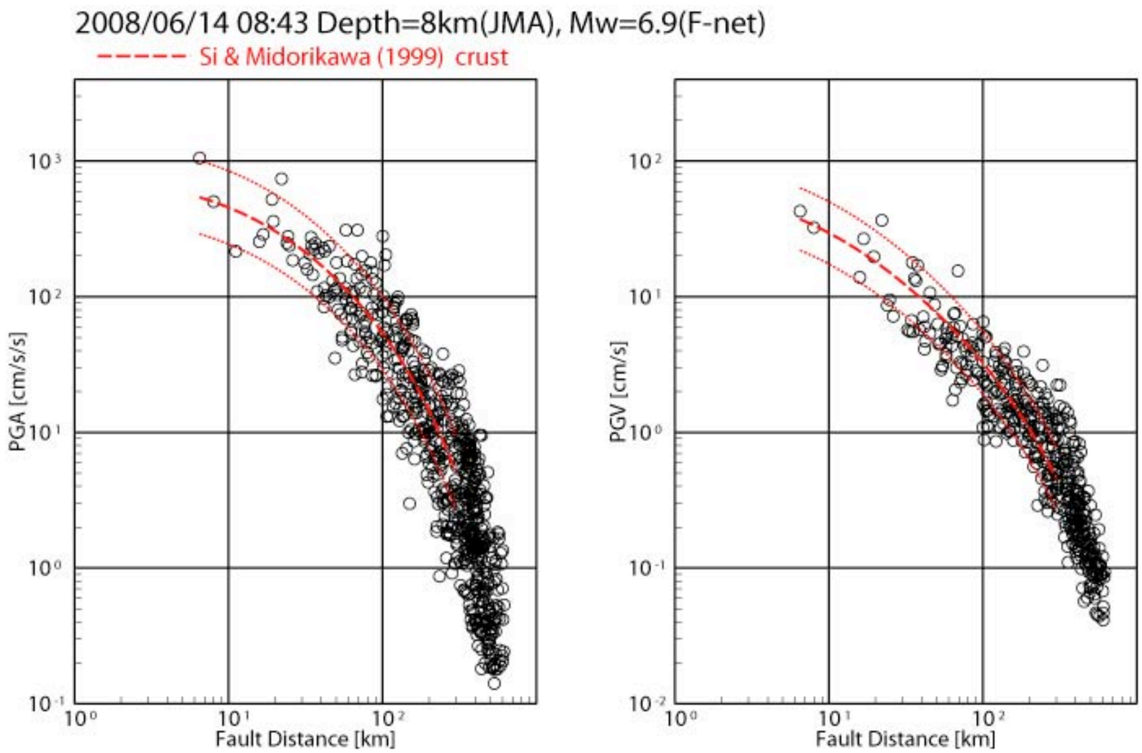

Figure 2.4. Comparison of recorded peak horizontal acceleration and velocity with the empirical ground motion model of Si and Midorikawa (1999) for crustal earthquakes. The solid line shows the median of the predictive model and the dashed lines show one standard deviation above and below the median. Source: NIED (2008).

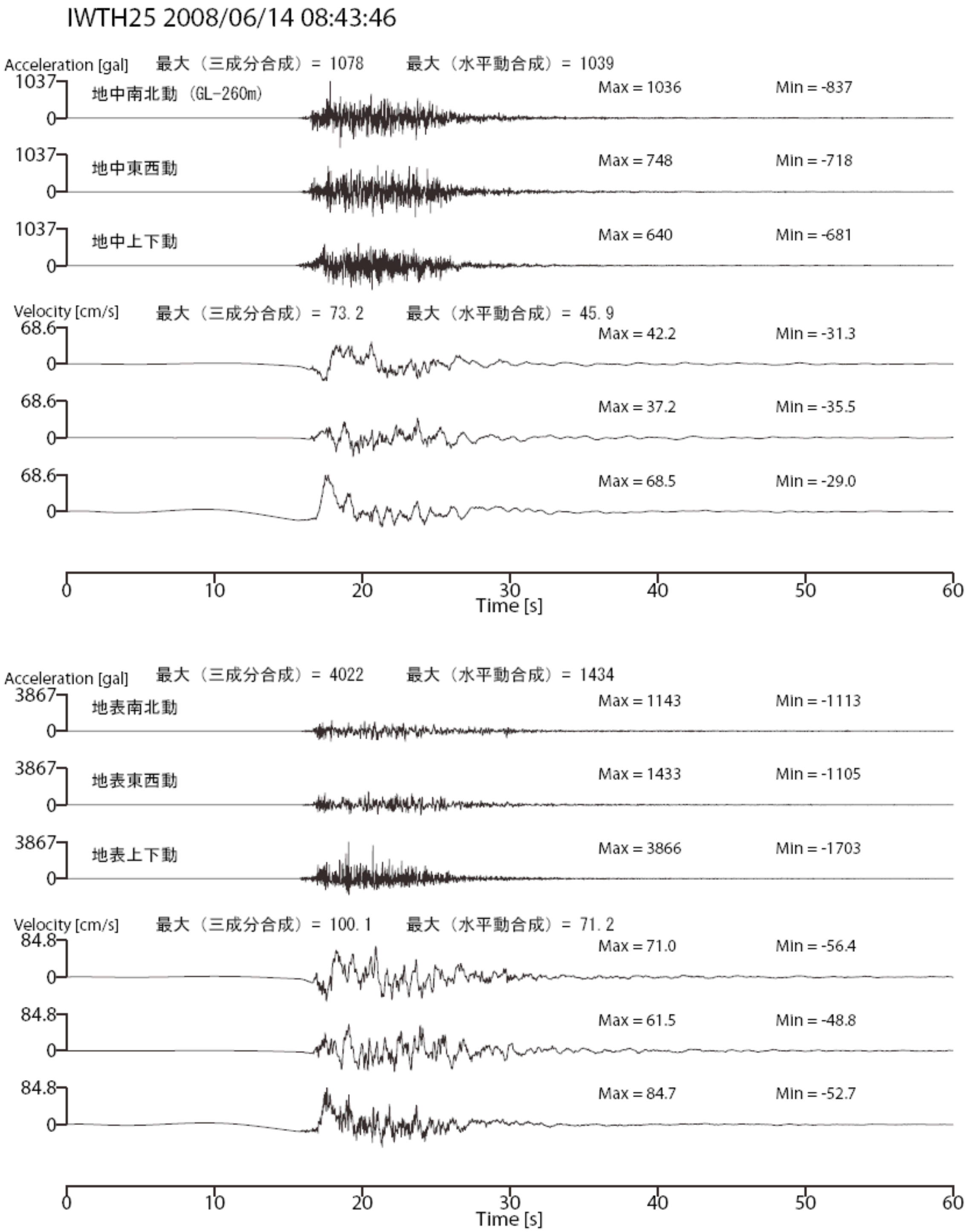

Figure 2.5. Recorded acceleration and velocity time histories at station IWTH25 at a depth of 260 meters below the ground surface (top) and at the ground surface (bottom). Source: NIED (2008).

Section 3 - Surface Fault Rupture

The 2008 Iwate-Miyagi Nairiku earthquake generated several surface fault related features along a 20-km long NNE-SSW stretch from Kunimiyama (Ikawa ku) in the North to Aratosawa Dam in the South. The fault feature locations compiled by the Active Fault Research Center [2] (here after AFRC) are shown in Figure 3.1. Some of these features were visited by GEER team members, however, the team was not able to visit all of them. Descriptions of some of the surface fault features are provided below. In these descriptions, the site location numbers provided in Table 3.1 and shown in Figure 3.2 are referenced. While surface fault features were observed by the AFRC at more than 10 separate locations, most of them occurred in sparsely populated areas and had minimal impact on engineered structures. However, the fault features observed in this earthquake do not plot on top of any of the previously know faults in the area (refer to Figure 3.2).

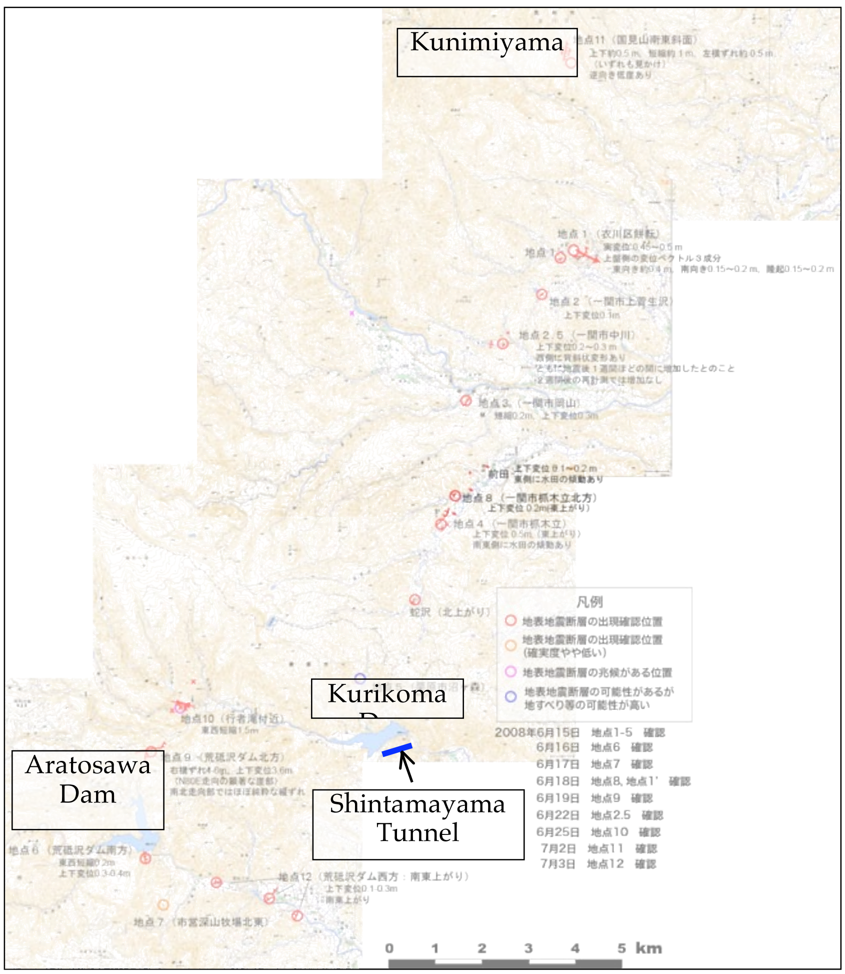

Figure 3.1. Locations of ground features related to surface fault rupture and related phenomena. (after [2], [4]).

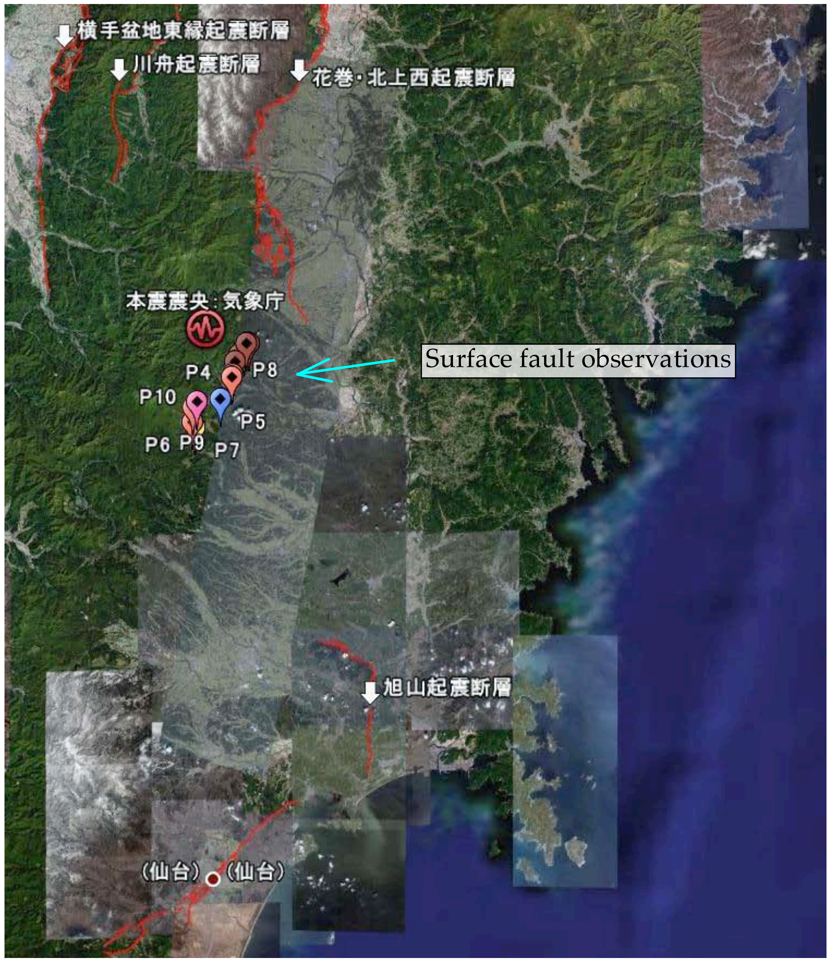

Figure 3.2. Surface fault observations from the Iwate-Miyagi Nairiku earthquake plotted on a Google Earth map with previously known active faults (red lines).

Table 3.1 Locations and types of surface fault related damage.

Point number, Location	Damage description
1, Mochikoro bridge	Asphalt pavement pushed up against bridge (Figure 3.5).
3, Ichinoseki City Okayama	A concrete canal (Figure 3.7) was cracked and a water pipe was broken.
9, North of Aratosawa dam	Strike-slip trace with right lateral displacement of 4-6 meters and vertical displacement of 3.6 meters.
9, South of Aratosawa dam	Spillway concrete structures damaged and road damaged in 3 locations (Figure 3.9 - Figure 3.12).

Point 1, Mochikoro bridge in Ikawa ku, Oshuu City

At Mochikoro bridge in Ikawa ku, Oshuu City (point 1), a surface fault trace appeared in a rice field following the earthquake (see Figure 3.3 and Figure 3.4). At point A (yellow mark) in Figure 3.3 the asphalt pavement was pushed up against the north abutment of the Mochikoro bridge and may be a compressional feature of the fault displacement. Latitude and longitude values for the four sites

Figure 3.3. Map of Mochikoro bridge area (bridge in orange color, surface fault trace in red). (After [2])

Figure 3.4. Looking east from the south end of the bridge at Surface fault trace at Oshuu City, Ikawa Ku, Mochikoro bridge. (Photo by Jörgen Johansson.)

Figure 3.5. Asphalt pavement pushed up against bridge abutment.

Point 3, Ichinoseki City Ookayama (38°58'23.2"N, 140°56'2.3"E)

At point 3, Ichinoseki City Ookayama (□□□□), an underground water pipe was broken [3] and concrete canal was damaged (see Figure 3.7). According to the AFRC some buildings were also damaged just north of National Road

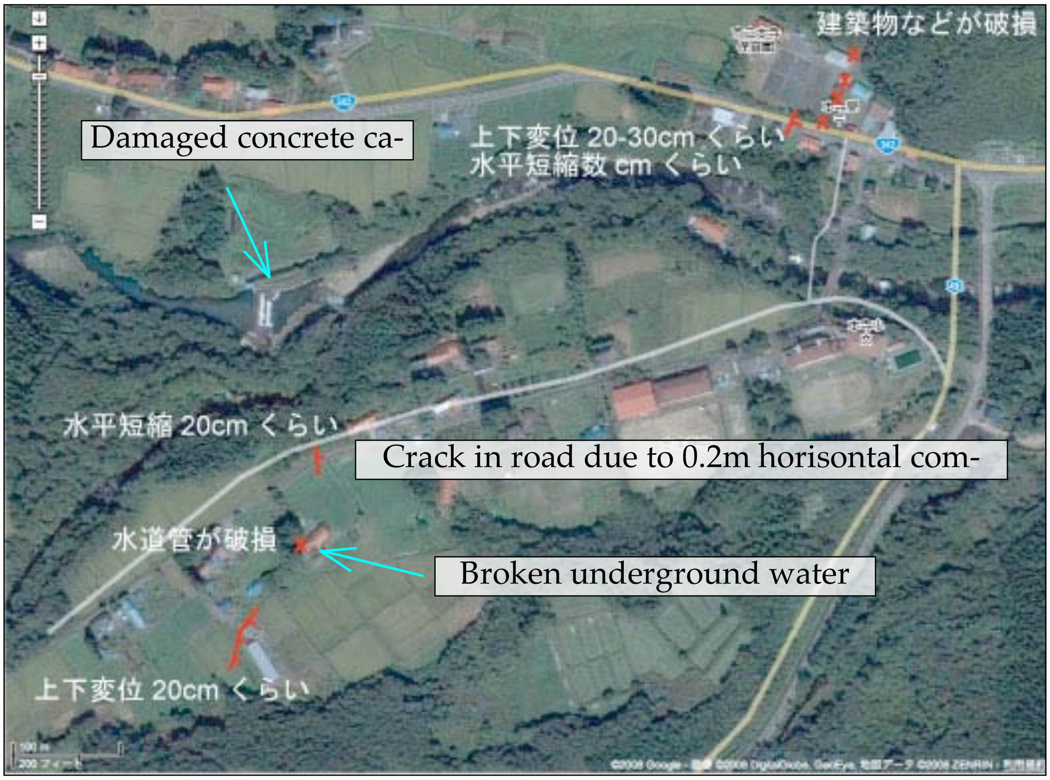

342.

Figure 3.6. Point 3, Ichinoseki City Ookayama. Surface fault damaged a concrete canal and broke a underground water pipe.

Figure 3.7. Concrete canal broken by surface fault. (photo by [5]).

Point 9, Aratosawa dam

At Aratosawa dam (point 9) a strike slip fault trace was discovered very close to big landslide that is described in section ??. Acoording to the Active Fault Research Center this is a fault induced surface feature, which can not be explained by landsliding. Thus if this was a fault, then how it may be related to triggering the large landslide needs to be clarified. Just south of the dam office, on the road to the dam office, there are 3 locations with road damage (see Figure 3.9) due to 0.2m east-west compression and 0.3-0.4m vertical displacement (see Figure 3.10). As seen in Figure 3.10 the deformations are quite large, but a concrete ditch next to the road did not crack at all. We could not find any crack in the surrounding ground and the retaining walls above the road (see Figure 3.9) suffered no damage, which is quite mysterious. On the other hand, just north of this location (see Figure 3.11) a concrete retaining wall suffered compression and shearing. The close-up in Figure 3.12 shows how the upper part of the retaining wall moved outward.

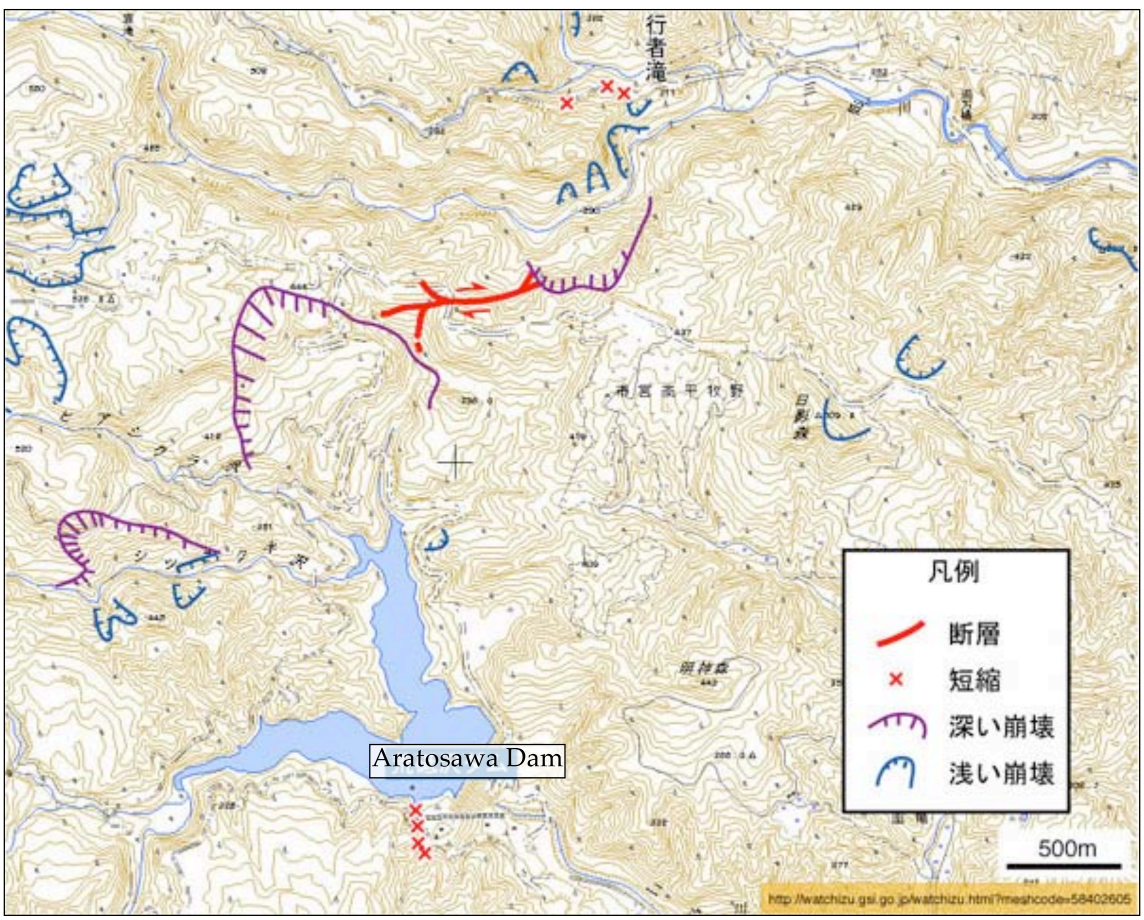

Figure 3.8. Map with landslide escarpment and surface fault (after [2]).

Figure 3.9. Aerial photo of 3 road cracks. The right most road damage is shown in Figure 3.10. Close ups of the area in blue rectangle are shown in Figure 3.11 and Figure 3.12.

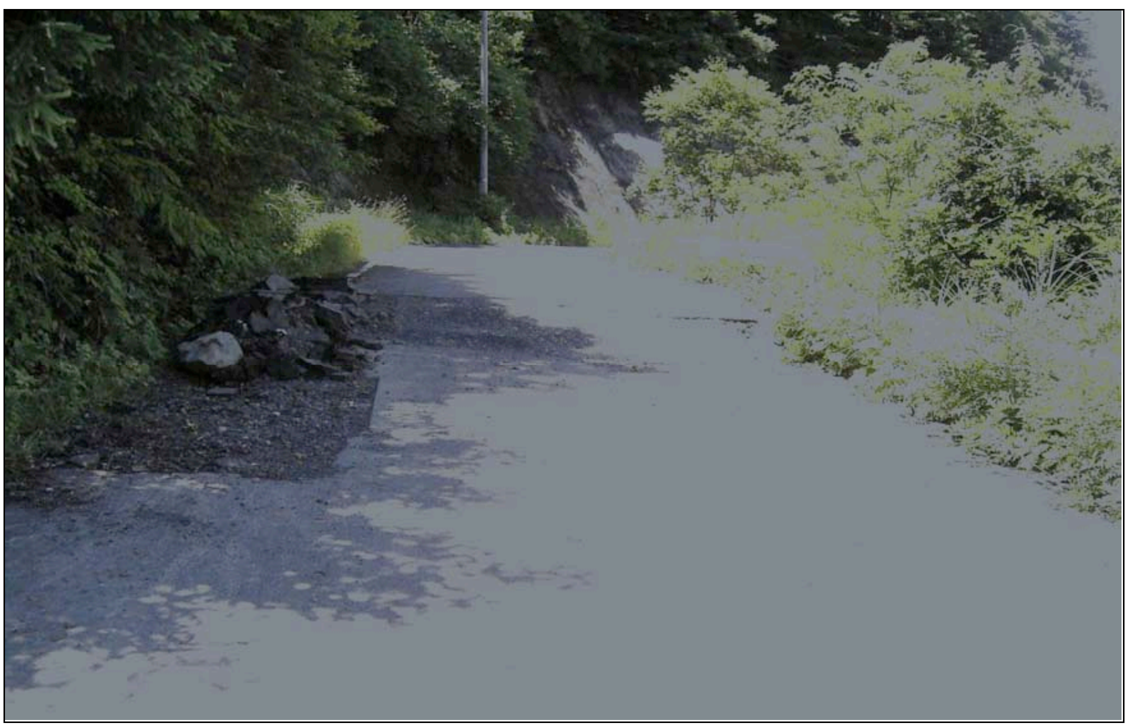

Figure 3.10. Road damage due to surface faulting (?) just south of Aratosawa dam. See text for explanation of question mark. Observe the bent guard rail.

Figure 3.11. Spillway Concrete structures cracked by ground deformation possibly related to surface faulting. Blue lines and boxes mark cracks. Dashed thin white line marks location of close-up photo in Figure 3.12.

Figure 3.12. Close up of cracked concrete retaining wall structure. Blue circles mark the sense of movement. The upper part of the retaining wall moved outward some 10 cm.

Shintamayama tunnel (East Mouth at N 38 54′ 2″, E 140 55′ 23″)
The Shintamayama tunnel is located some 20km to the east of Ichinoseki City, on prefectural route 42, just to the south of the Kurikoma dam (see Figure 3.13). The 1220 m long 10.25m wide, and 4.7m high tunnel consisted of 97 12.5m long segments (see Figure 3.15). It sustained cracks some 20 mm wide at 250m, 1-3 mm at 400m, and cross section compression at 600m (segment 20, 32, 48) from the East mouth respectively, shown by red marks in Figure 3.13 and in detail in Figure 3.15. A detail of the cracks at segement 20 and 21 are shown in Figure 3.14. There most of the cracks were extensional. Blue arrows show that the eastern segment moved down with respect to the western segment, while red ones show the opposite. Numbers in parentheses show these relative displacements in mm. The 50 meter portion closest to the east mouth was extended with openings 5mm up to 2cm wide between the segments (see Figure 3.15.)

We also went on top of the hill , through which the tunnel crosses, however we found no cracks or other signs of major landsliding and/or surface faulting. (Figure 3.16 shows the GPS tracks.) There was only some shallow surface failure and stones that had jumped out of their locations. As of this writing it seems that the induced damage is more likely due to a landslide as indicated with blue dashed line in Figure 3.13, than related to the a possible surface fault. Therefore if the cause is a deep-seated landslide, long-term monitoring will be a must for rational repairs.

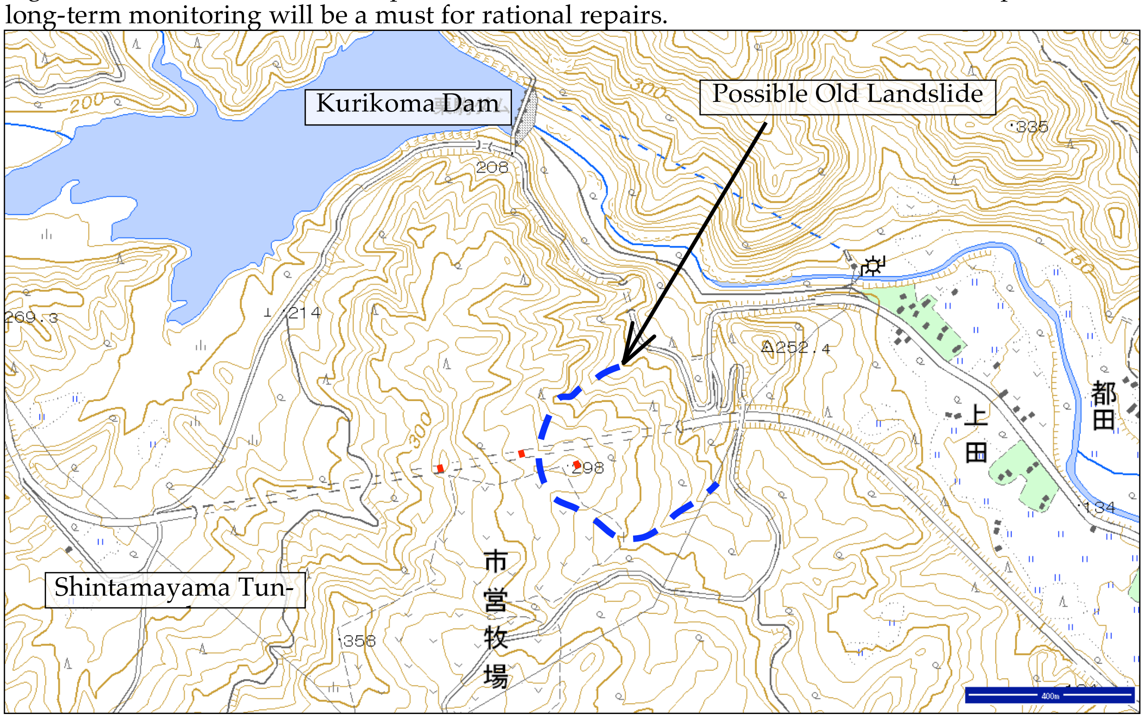

Figure 3.13. Shintamayama tunnel with possible old landslide that may have been reactivated. The red marks show major crack locations, at 250m, 400m, 600m (segment 20, 32, 48) from the East mouth respectively.

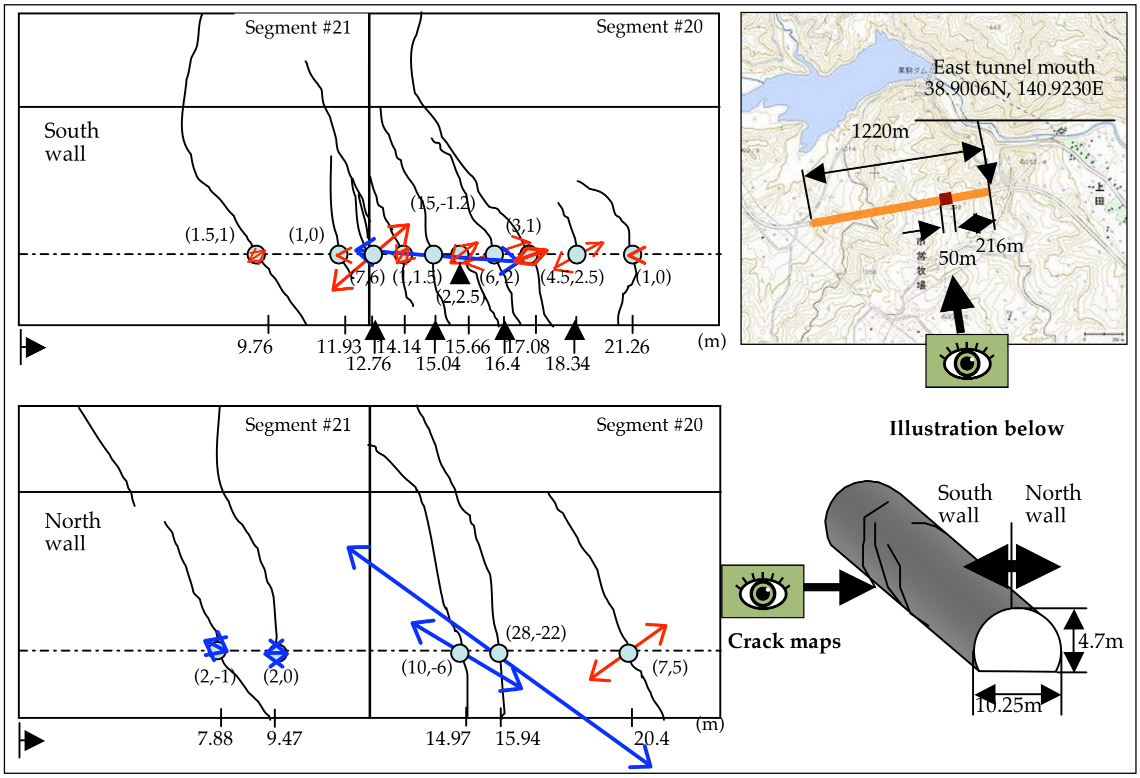

Figure 3.14. Cracks in Shin-Tamayama Tunnel: A 36m-long segment 216m inside the eastern mouth (38.9006N, 140.9230E) of the total 1220-m-long tunnel was diagonally cracked. The above two figures show projections of the cracked south and north walls on a virtual screen put north behind the tunnel.

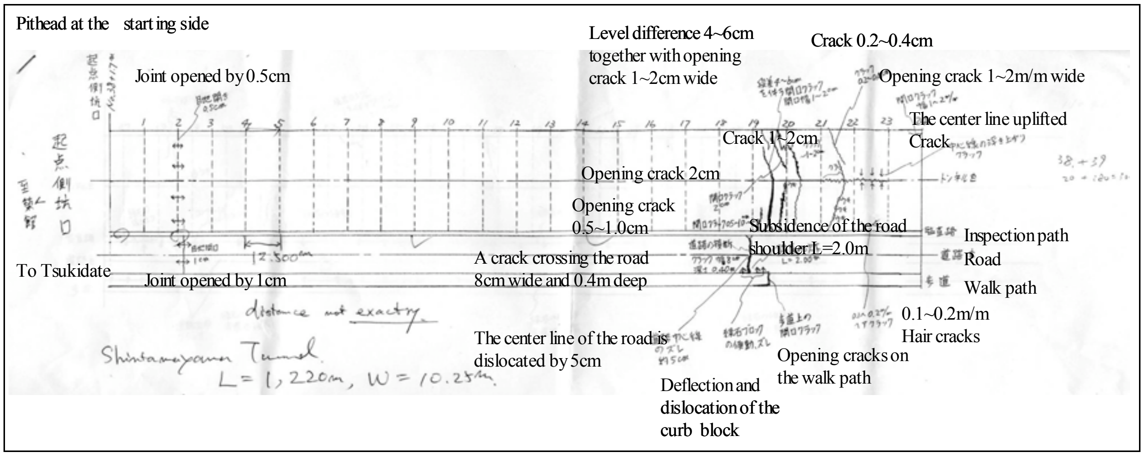

Figure 3.15a) Crack map segement 1-24 of shintamayama tunnel. Crack map provided by local reconstruction engineers

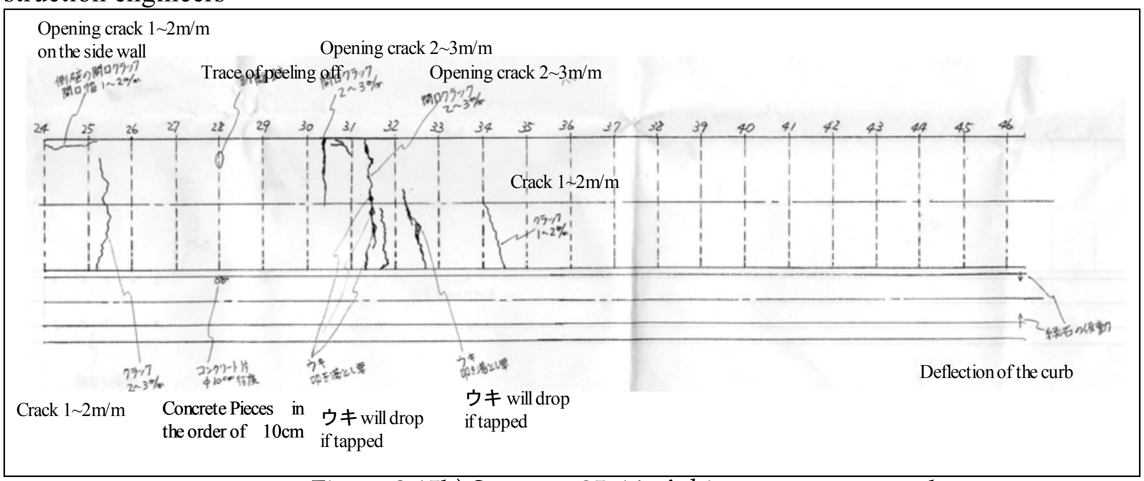

Figure 3.15b) Segment 25-46 of shintamayama tunnel.

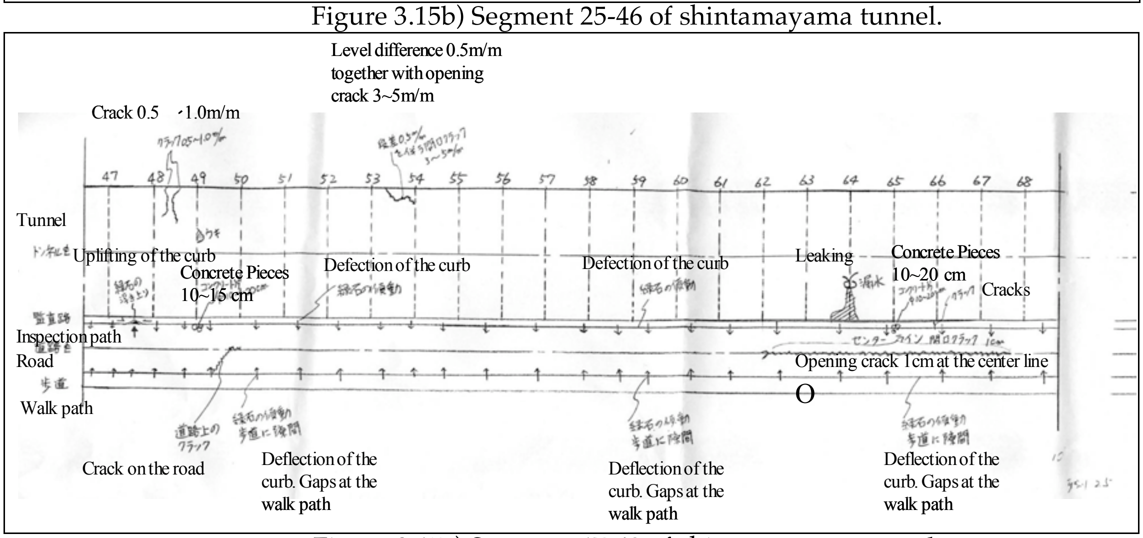

Figure 3.15c) Segment 47-68 of shintamayama tunnel.

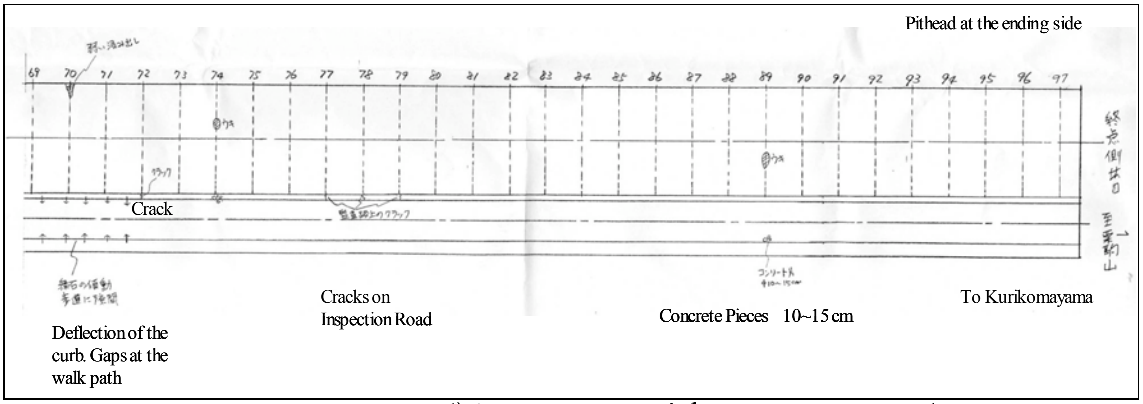

Figure 3.15d) Segment 69-97 of shintamayama tunnel.

Figure 3.16. Google Earth view of Shintamayama tunnel (white dashed line) with GPS tracks in light blue. We found neither major slides nor any fault offsets.

Acknowledgment
We wish to thank Suzuki Takasuke for several explanations of the local geology.

References

1. Geographical Survey Institute, Digital Topographical Map of Japan,

http://portal.cyberjapan.jp/denshi/opencjapan.cgi?x=140.90625&y=38.89583333333333&s=10000

2. Active Fault Research Center, Quick Report on the 2008 Iwate Miyagi Nairiku Earthquake", (in Japanese), 2008, Web site last accessed August 5, 2008,□□□□□□□□□□□□
3. Active Fault Research Center, Urgent field investigation quick report No.6, (June 23 2008,) □□□□□□□□□□□□□2008.6.23□, Quick Report on the 2008 Iwate Miyagi Nairiku Earthquake", (in Japanese), 2008, Web site last accessed August 8, 2008, http://unit.aist.go.jp/actfault/katsudo/jishin/iwate_miyagi/report/080623/index.html
4. Active Fault Research Center, Map of Surface Fault Related Features, Downloaded on August 5, 2008. http://unit.aist.go.jp/actfault/katsudo/jishin/iwate_miyagi/080709_1map.pdf
5. Ishiyama et. al. ,The 2008 Iwate Miyagi Nairiku Earthquake Fault investigation No. 2, Geomorphology Laboratory, Institute of Geography, Department of Geoscience, Tohoku University, http://www.dges.tohoku.ac.jp/~geomorph/08iwatemiyagijisin/jishinsokuhou2dan.html

Section 4 – Landslides

The earthquake occurred in an interior and rural mountainous region of Tohoku, Japan. Within 20 kilometers of the epicenter, in the steep terrain of the mountains and coarse valley fill of the small agricultural valleys, landslides were ubiquitous. Surprisingly, there were no observations of liquefaction from this event of any significance. Landslides caused by the earthquake were primarily deep-seated rotational slides in weathered bedrock; collapses of corner buttresses composed of both rock or weathered rock and soil; rockfall and rock avalanches; shallow translational slides and shallow debris flows. Shallow regolith slides of soil and weathered material sliding on top of more competent bedrock were common at road cuts and a occasionally mobilized into debris flows that carried material to stream valley bottoms.

The Iwate-Miyagi Nairiku earthquake follows several other damaging earthquakes in the Tohoku region of Japan in the last four years. The landslide density of this event was far less than occurred during the Niigata Chuetsu earthquake of 2004 that devastated the Uonuma Hills area east of Nagaoka, Niigata. However, it had comparable landslide density to the Niigata Chuetsu-Oki earthquake of 2007. The principal difference between this year's event and the event of 2007 was that the Iwate Miyagi-Nairiku event had an onshore shallow focus and surface rupture that resulted in severe landsliding damage close-in to the epicenter. During the 2007 event, the focus was offshore and the observable damage was at a minimum of 10 km east of the epicenter on the coast of Kashiwazaki and Kariwa.

One particularly enormous event was a 50,000,000 m^3 landslide that entered the Aratozawa Dam reservoir. This feature has a headscarp in the vicinity of and associated with the surface fault rupture. Numerous other large landslides occurred in this 10-kilometer zone around the earthquake epicenter.

Landslide damage during this earthquake was observed equidistant to the epicenter in all directions. Based on our observations, presented in the Google Earth map, catastrophic landslides that collapsed large portions of mountainside and destroyed highways and bridges occurred within 15-20 kilometers of the epicenter. Most landslides were observed within a radius of 22 km of the epicenter. Virtually all damage of significance was observed within a radius of 35 km of the epicenter (Figure 4.1). Landslide damage was isotropic about the epicenter with the exception of the large alluvial fan west of Mizusawa City, that is a relatively flat lowland area of farms.

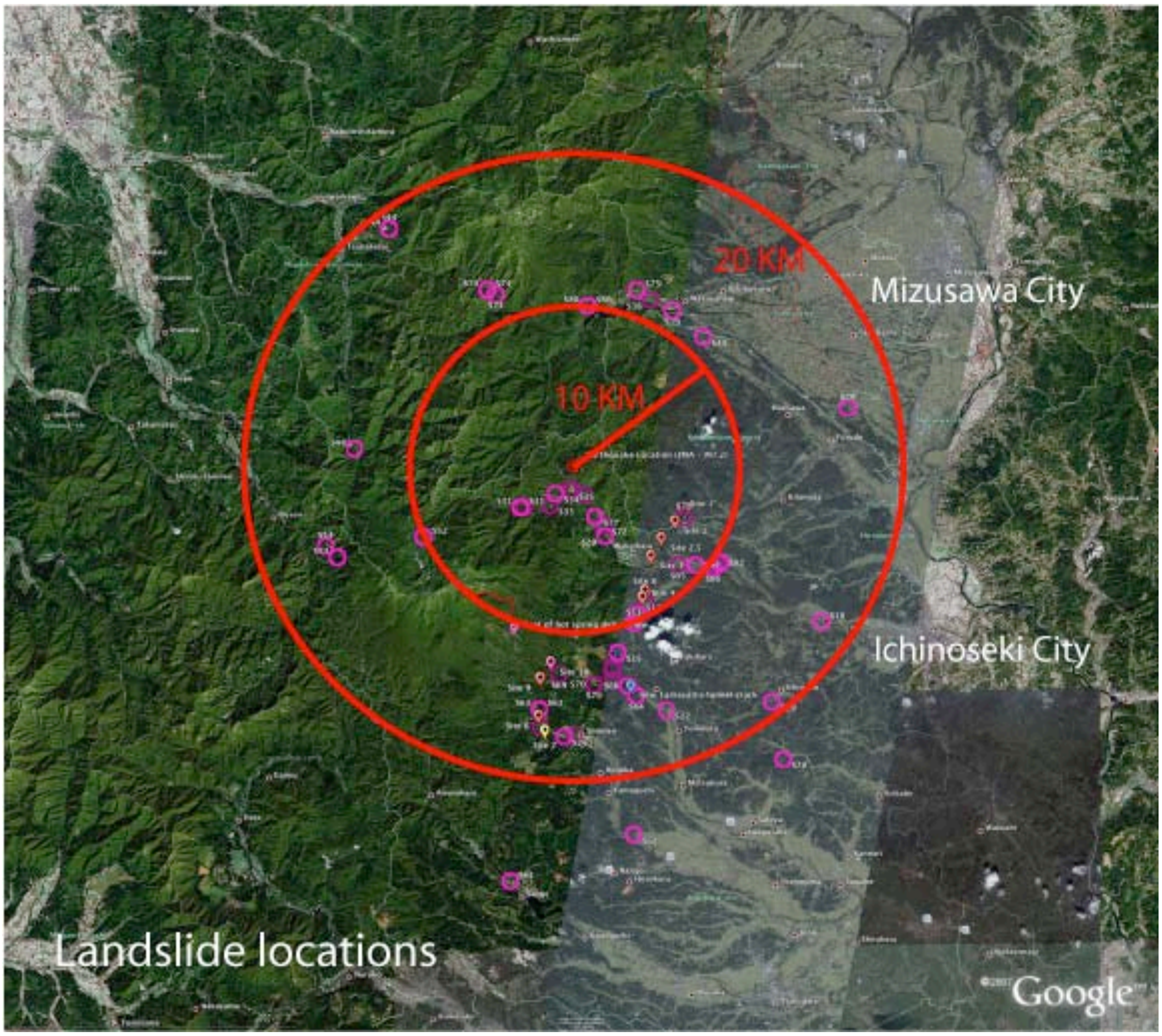

Figure 4.1: Map of observed landslide damage. All significant landslide activity during the earthquake was within a radius of 22 kilometers of the event epicenter.

Landslides were the principle cause of the road closures in Iwate, Miyagi and Akita prefectures. Route 342 was directly above the epicenter in the vicinity of landslides that effected the route around Shiyou Yuyama onsen (Site 31-35). The highway in this area suffered a large number of large landslides that swept away numerous portions of the road, as well as brought down a large steel frame bridge (Site 36). Highway 397 to the north, suffered for large landslides close to the epicenter. These Landslides severed transportation between southern Akita and Iwate prefectures. Landslides also closed most highway routes in the northwestern corner of Miyagi Prefecture. The reconnaissance team was able to access most of at the central region by entering from all directions to the point of road closures. We were able to get government permission to pass many road closure points and access the landslide failures directly. At a number of dam reservoir sites, landslides entered the reservoir, elevating the water level and in at least one case sent a wave of water over the spillway.

The following examples are representative of the types of landslides that occurred in the central region. A more thorough listing of landslides observed from the air and on the ground can be seen in the Google Earth site companion to this report.

1: Deep rotational landsliding in weathered bedrock

Aratozawa Dam, Miyagi Prefecture: The volume of the landslide entering the Aratozawa reservoir is believed to be about 1.5 million cubic meters, entering approximately 500 meters beyond the pre-event shoreline of the north arm of the reservoir. The total volume of the slide is estimated at 50 million cubic meters (Figure 4.2). This slide is comparable to the giant landslide that occurred near Yamakoshi Village in the Uonuma Hills of Niigata during the 2004 Niigata Prefecture Chuetsu Earthquake (Refs. ES 2006, 6ICGCHE). The Aratozawa landslide was a deep translational slide in steep terrain with a large runout of disintegrating material at the toe. The landslide was composed of weakly cemented weathered volcanic ash, and volcanoclastic material. The height of the headscarp varies from 50-150 meters in height. The landslide extends about 1.2 kilometers in length, and is on average 800 meters wide. The depth is estimated to average 50 meters. More detail regarding the Aratozawa Dam, landslide and seiche are provided below.

Large rotational slides caused the impounding of nearly a dozen small quake lakes behind debris that blocked valleys and formed natural dams. Quake dams formed on the Sanhasamagawa river and the Nihasamagawa river, five formed on the Hasamagawa river in Kurihara, Miyagi Prefecture, and four on the Iwaigawa river near Ichinoseki, Iwate Prefecture. Most of the lakes are 100 to 200 meters wide.

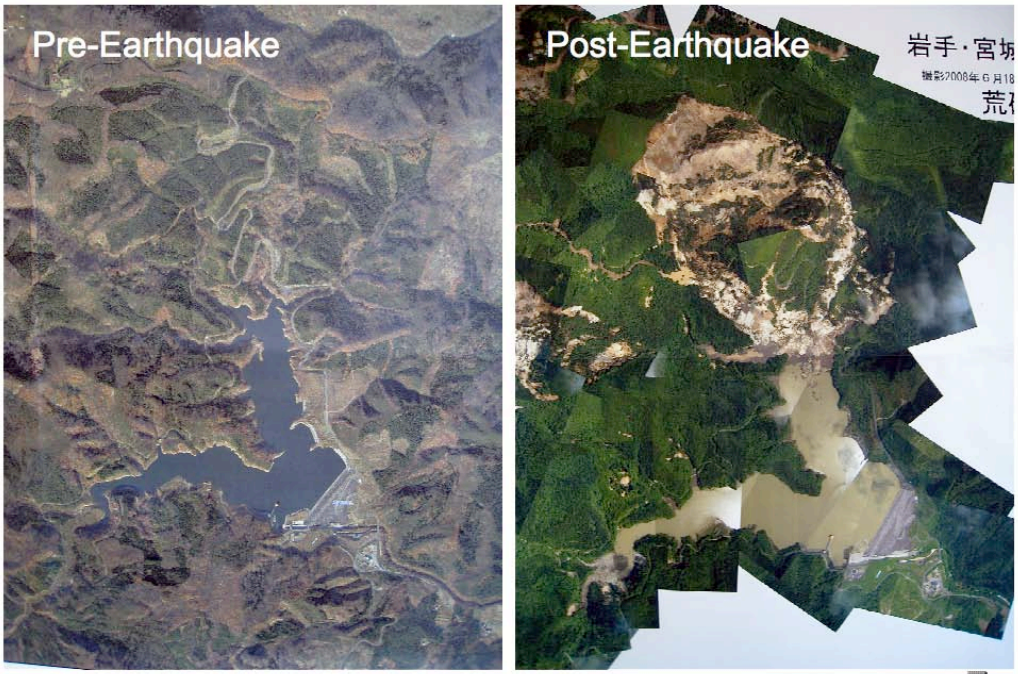

Figure 4.2: Aratozawa dam and reservoir prior to, and after, the earthquake (Site S27, N38.8837° E140.856°, 6/27/08 17:00).

2: Rockfall and Rock Avalanches

Near Mt. Kurikoma at the Komanoyu Onsen near the head of Route 457 in Kurihara, Miyagi Prefecture, along the border of Iwate Prefecture, several large rock avalanches were loosened by the earthquake. One of these landslides struck the Onsen killing one of the owners and several guests. The reconnaissance team was able to access the downslope end of the rock avalanche that was composed of large blocks up to house size that crossed route 457 (Figure 4.3). In Iwate Prefecture, failure of a rock mass collapsed a large steel frame bridge on route 342 (Figure 5.8). Rockfall was typically associated with extremely steep terrain and cliffs in excess of 50° (Figure 4.4).

Figure 4.3: Rock avalanches on Route 42 west of Numano-Mori Mountain.

Figure 4.4: A moderate sized rockfall closed route 37 at Site 40. The slide contained car sized boulders of weather rock (Site S40, N39.0993° E140.97252°, 6/28/08 12:08).

3: Shallow regolith landslides

Shallow landslides were observed in colluvial or residual soils of 1 m to 3 m depth and ranged from 50 m^3 to several thousand cubic meters in volume. Small isolated debris flows were uncommon. Typical slope surface and failure plane inclinations were 50°–70°, failing in translation as debris slides and slumps. These types of landslides were of sufficient size to close all major transportation routes in the epicentral region. An example of a shallow regolith slide can be seen at Site 31 where a thin veneer of slope material mantling bedrock slid across route 342, Iwate Pref. (Figure 4.5). This landslide carried both lanes of Route 342 down into the river below the slope. Failures like this were common within 20 kilometers of the epicenter.

Figure 4.5: A large but shallow regolith slide of weathered soil closed a portion of Route 342, Iwate Prefecture (Site S31, N39.00532° E140.84219°, 6/28/08 9:45).

4: Man Made Embankments

Route 49 at Iwate Miyagi Prefecture border

Embankment failures were almost entirely associated with road transportation and were typically seen at switchbacks, on fills crossing hillslope depressions, and stream-culvert crossing road fills (Figure 4.6). No train routes crossed the epicentral region. Minor embankment failures resulted in many tens of kilometers of pavement damage to roads, typically failing into the downslope open space. Where embankment failures were severe, entire road beds slid into adjacent stream valleys or depressions. Manmade embankment failure of road beds was the primary cause of road closures. Typically, deformations were observed on the down slope side of cut and fill construction on mountain slopes. Where embankments elevated the roadbed above surrounding terrain, deformations were more uniformly distributed across the embankment.

Figure 4.6: Site 79 A typical small embankment failure along Route 342. Photograph courtesy of the Iwate Prefecture Government Office, Morioka, Japan.

Settlement of embankments at bridge approach fills was common, and created a step at the bridge abutment of up to 30 cm. Differential settlement at bridge abutments hindered traffic and emergency response immediately after the earthquake. These conditions are dangerous in the immediate aftermath of an earthquake. Differential settlement was remedied when emergency road crews that placed gravel fill at the abutment step and marked the site as a hazardous road condition. An independent section on damage to the transportation network can be found in Section 5 of this report.

Reservoirs and dams performed well during the earthquake. No dam suffered vertical deformations or lateral displacement in excess of 1.5 m, and in no case did water cross the crest of any dam despite numerous cases of landslides entering lakes at high velocity. A report on dams and reservoirs can be found in Section 6 of this report.

Figure 4.7. Landslide at Aratosawa dam: Aerial photo of the largest landslide with Kurikoma Volcano rising behind. The terrain here is suggestive that similar historic landslides have been reactivated. A large and almost horizontal laminated structure of lose volcanic sands and ashes is being exposed on the escarpment. When wet, some pieces of light-gray

rock fragments taken at the toe of the landslide mass smelled strongly of hydrogen sulfide [1].

5: Detail discussion of Aratosawa Dam and landslide induced Seiche

In the Iwate-Miyagi Nairiku earthquake of June 14 2008 a large landslide of some 50 million cubic meters caused a seiche several meters high when some 1.5 million cubic meters slid into the dam lake. The seiche flowed into the spill way but did not flow over the dam crest.

The road locations after and before the earthquake were drawn upon the DEM (Figure 4.11) by using images from the helicopter survey, photos, and a field GPS survey (open circles) etc. The black arrows show that Points P1 P2 and P3 have respectively moved about 200m, 300m and 500m SSE towards the dam lake. The slid blocks are lined up in a succession. The cross-section A-A' in Figure shows a gradient of about 3-4 degrees. Even though the base slope was very gentle the soil masses have moved some 200 to 500 meters. (Aero Asahi Co. provided the digital elevation model). Between June 15 and July 19 deformation were still going on and a new large scarp appeared behind point A in Figure 4.11).

Figure 4.8. Location of the Aratozawa dam site in Kurikomabunji, Kurihara city, Miyagi Prefecture (宮城県栗原市栗駒文字).

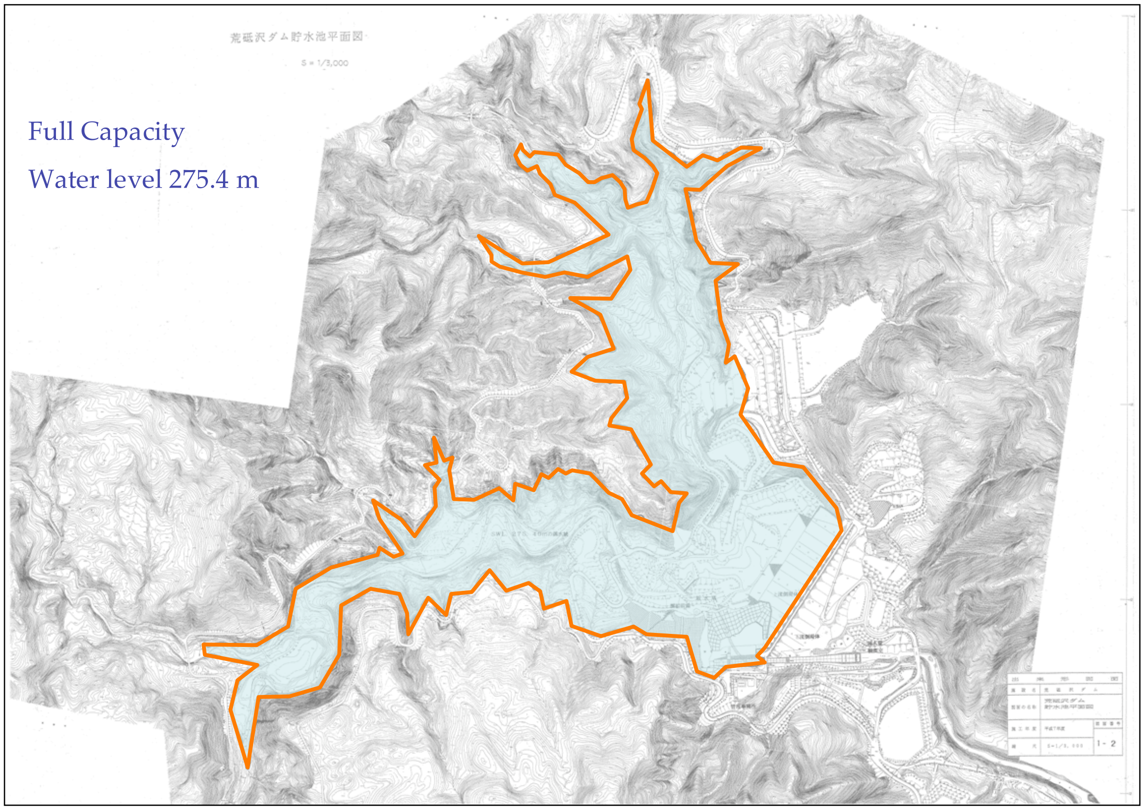

Figure 4.9. Aratozawa dam lake (”Indigo dye lake”). Orange line shows the full capacity water level of 275.4 m. Figure 4.9 Shows a topographic map prior to the filling of the lake with the full lake elevation, 275 m, marked with an orange line.

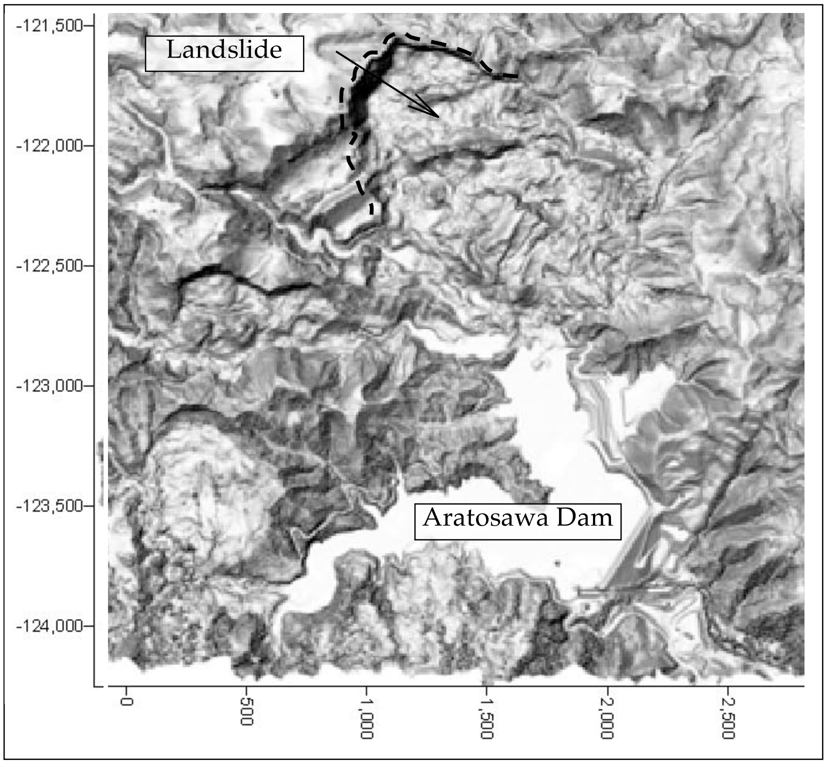

Figure 4.10. Laser scan of Aratosawa dam and landslide area. (Aero Asahi Co. provided the digital elevation model). Figure .10 shows a laser scan of the Aratosawa dam and landslide area provided by the Aero Asahi Co. The coordinates are based on the JGD10 Grid. They numbers are in meters. The y-axis numbers have a -1 cut of from the left side, i.e. 23,500 should be -123,500 etc.

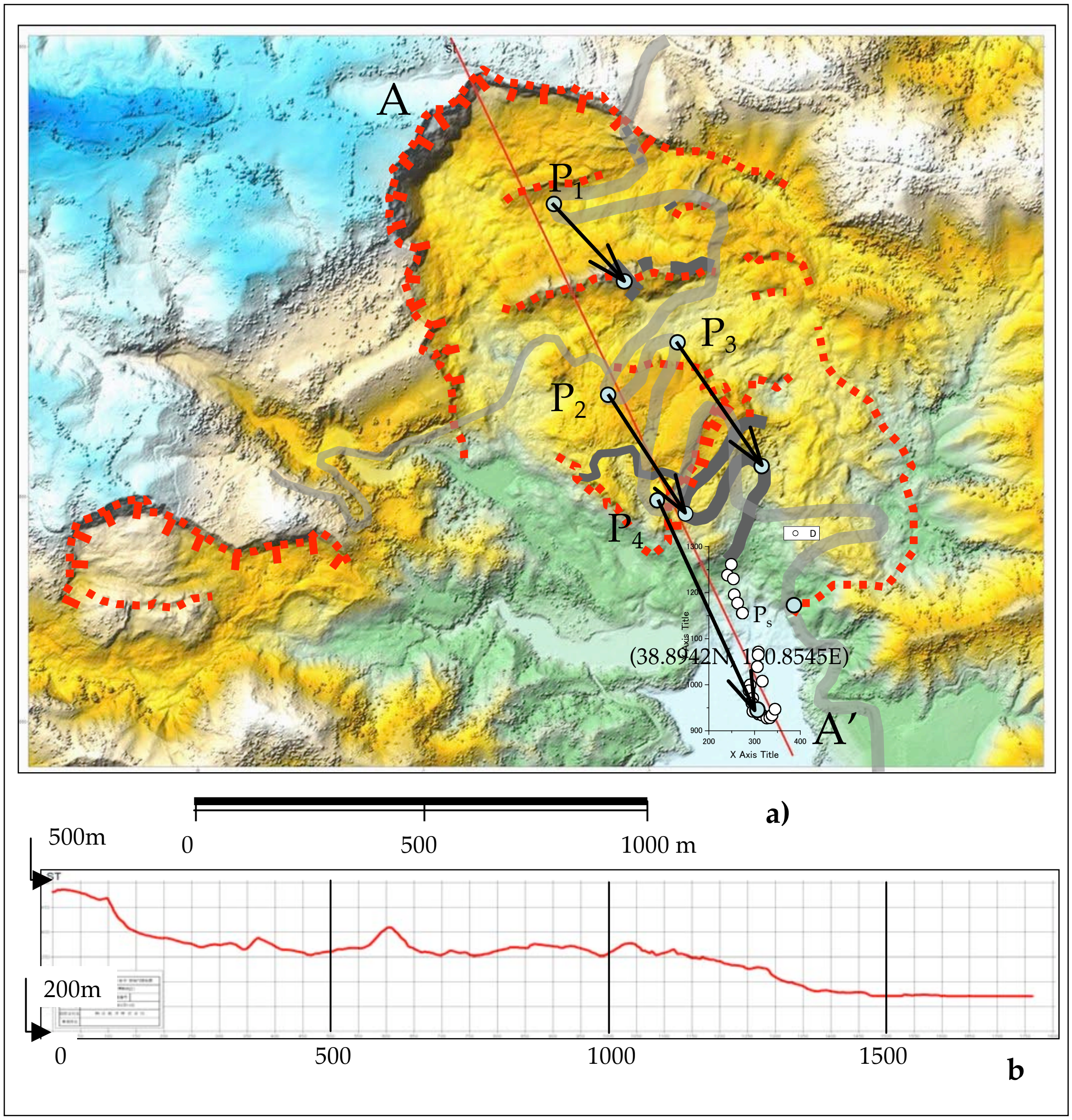

Figure 4.11. Landslide at Aratosawa dam. The road locations after and before (gray) the earthquake drawn upon the DEM. Even though the base slope was very gentle the soil masses have moved some 200 to 500 meters. (Aero Asahi Co. Provided the digital elevation model).

Landslide induced seiche

We measured the seiche high water marks on July 13 and 25. Table 4.2 gives lake water elevations as measured by dam management office and Table 4.3 gives coordinates and seiche heights in meters with respect to the lake elevation before the earthquake (268.5m.)

Table 4.2. Dam Lake elevations measured by Dam Managament Office.

Date	Elevation [m]	Remark
June 14 2008	268.5	Before Earthquake
June 14 2008	270.9	After Earthquake, water level increased due to landsliding and possibly due to tectonic deformation
July 12 2008	261.4	Reference elevation for measurements on July 12
July 13 2008	261.2	Reference elevation for measurements on July 13 (Lake is being emptied slowly)

Table 4.3. GPS data and seiche height above lake elevation before earthquake for July 13 and July 25.

Point Id	Latitude	Longitude	Height above lake elevation before earth-quake [m]	Time
30000	38 53 28.9	140 51 18.7	8.7	July 13
30000	38 53 28.4	140 51 17.0	4.2	July 13
30000	38 53 24.3	140 51 20.1	8.5	July 13
30000	38 53 35.2	140 51 16.1	4.1	July 13
30000	38 53 34.2	140 51 16.1	5.5	July 13
30001	38 53 33.4	140 51 16.1	6.1	July 13
30001	38 53 1.6 N	140 50 25.6	4.5	July 13
30001	38 53 4.7 N	140 50 28.7	3.7	July 13
30001	38 53 7.9 N	140 50 31.3	7.7	July 13
30001	38 53 4.8 N	140 50 32.4	3.2	July 13
30001	38 53 10.6	140 50 51.4	4.2	July 13
30001	38 53 10.6	140 50 52.8	4.5	July 13
194	38 53 36.4	140 51 06.5	9.35	July 25
196	38 53 33.4	140 51 04.0	7.25	July 25
197	38 53 32.1	140 51 03.9	7.35	July 25
198	38 53 31.1	140 51 04.8	5.95	July 25
199	38 53 30.7	140 51 05.1	6.55	July 25
200	38 53 29.5	140 51 06.4	4.15	July 25
201	38 53 28.9	140 51 05.8	6.35	July 25
202	38 53 27.0	140 51 04.6	7.75	July 25
203	38 53 26.8	140 51 05.0	6.75	July 25
204	38 53 26.8	140 51 07.2	5.15	July 25
205	38 53 26.3	140 51 06.8	5.75	July 25
206	38 53 25.7	140 51 07.1	6.85	July 25
207	38 53 25.0	140 51 06.9	5.85	July 25
208	38 53 23.4	140 51 06.9	5.25	July 25
209	38 53 22.8	140 51 07.6	6.45	July 25
210	38 53 22.4	140 51 07.9	7.25	July 25
211	38 53 21.0	140 51 09.2	5.45	July 25
212	38 53 20.1	140 51 09.8	6.25	July 25
213	38 53 18.9	140 51 09.8	7.45	July 25
214	38 53 19.0	140 51 10.4	7.75	July 25
215	38 53 18.5	140 51 10.9	8.05	July 25
216	38 53 18.0	140 51 11.8	6.35	July 25
217	38 53 17.3	140 51 13.8	4.95	July 25

A laser distance meter was used to measure height above the current lake elevation of high water mark traces, such as leaves and grass remaining in trees.

Figure 4.12. Recording locations of typical high water mark trace with GPS and laser distance meter.

As can be seen in Table 4.2 the lake elevation increased from 268.5 m before the earthquake to 270.9 m after the earthquake. The lake is as of this writing being emptied as to allow for inspection. The water level is now decreasing with some 15 to 20 cm/day. The difference in lake elevation before and after the earthquake is due to the landslide and possibly also due to some tectonic deformation. Out of the 50 million cubic meter large landslide some 1.5 million cubic meters was estimated to have entered into the lake, assuming the lake elevation increase was only due to the landslide.

The seiche heights (from Table 4.3) were plotted in Figure 4.13. We can see that on the right side in the Figure 4.13 (East side) the elevation increases from 4.1 meters to 8.7. On the Western side there is a zig-zag patterns of heights, whether this may be due to the topographical features of the lake border and/or due to error in our measurements. It is not always easy to find the highest high-water-mark in the field. At the far end, points 11,12, 14 in Figure 4.13, heights are lower, likely since here the seiche wave can can spread and run up long distances. However at point 13 which is close to a fairly steep location the seiche height reached 7.7m.

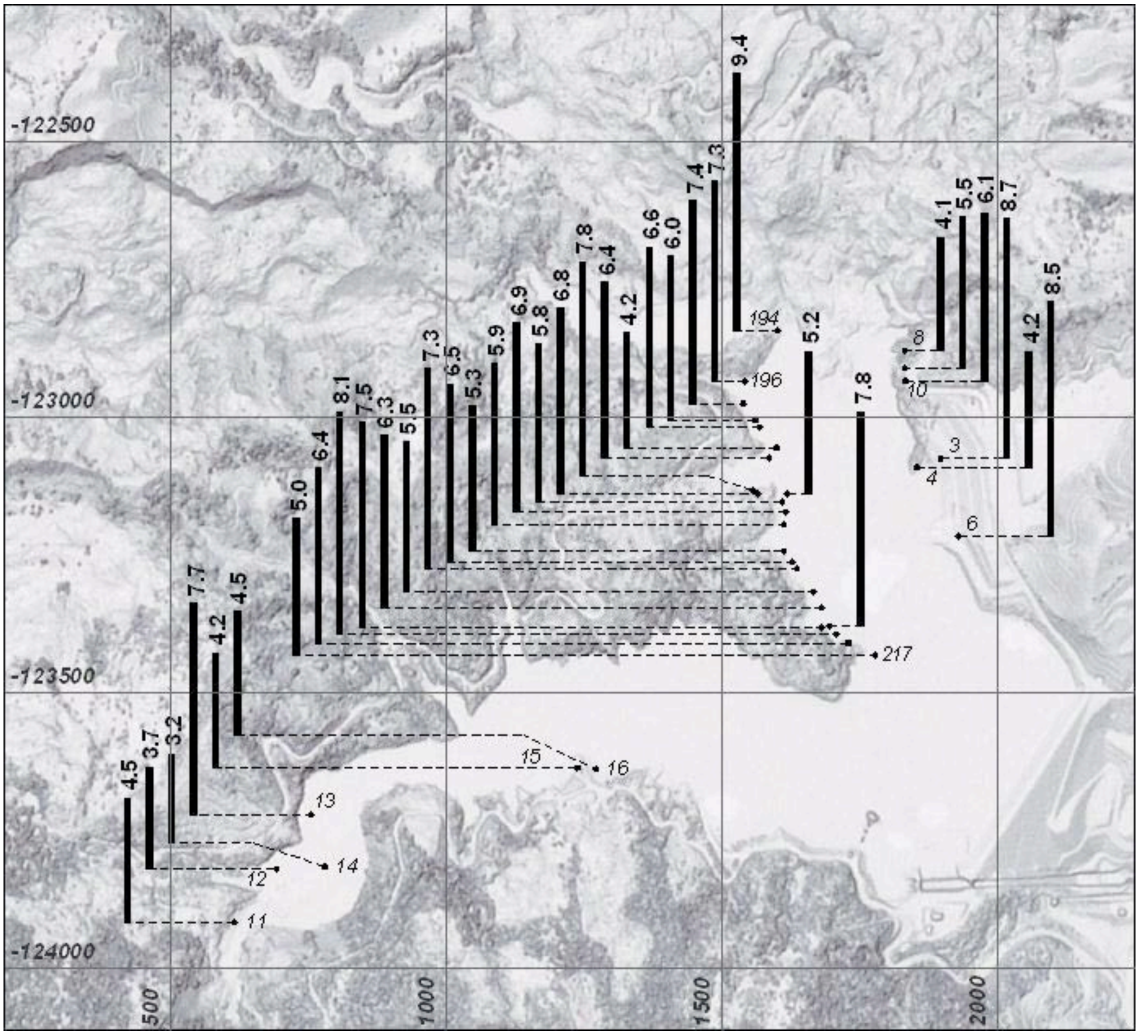

Figure 4.13. Seiche heights with respect to the pre-event lake elevation measured in the field on July 13 and July 25.

The seiche heights together with digital elevation models of the area before and after the earthquake serve as inputs to a shallow water wave propagation code, that Tokyo University hope to perform to back calculate the landslide velocity.. The landslide induced seiche brought sediment with it and deposited some material on the dam body as seen in Figure 4.14.

Figure 4.14. Sedimentation of fine particles on the lower part of the dam covers vegetation and indicates a minimum seiche height. Old reed grass in the top part of orange rectangle appear to have been deposited by seiche.

Acknowledgment

Yoshimitsu Tajima, Date, and Fujita for help with the Seiche survey. Edwin Leon for preparing Seiche figure.

References

1. Kazuo Konagai et. al. Quick report of the 2008 Iwate/Miyagi Earthquake (Ver 2.2), 2008

Section 5 – Transportation Systems

Roadway damage throughout the epicentral region was pervasive. The reconnaissance team tried to gain access to the center of the region from the North, South, East and West, yet progress was eventually halted on every roadway due to landslides or embankment failures that rendered the roads completely impassable. In some instances, landslide or rock fall debris covered the roadway blocking passage (Fig. 5.1 – Site S16 and Fig. 5.2 – Site S40), while in other cases the landslides had completely taken the road out and carried it downhill (Fig. 5.3 – Site S31). Embankment failures ranged from small cracks in the asphalt to large vertical and horizontal offsets caused by seismic compression and slumping (Fig. 5.4 – Site S2 and Fig. 5.5 – Site S34). These types of failures were too prevalent to document individually, however, pictures of some of the more severe damage and are linked to the GPS track logs in the accompanying Google Earth map. Settlement of approach fills leading to bridges (Fig. 5.6 – Site S48) was also common, along with some slope-type failures of steep embankments (Fig. 5.7 – Site S41).

Among the most notable roadway failures was the collapse of a large, two-span, steel girder bridge on Hwy 342 (Fig. 5.8 and Fig. 5.9 – Site S36). The collapse appears to have been primarily caused by large-scale lateral movement of the western slope abutment towards the river valley. This lateral movement was evident in severe road distress more than 100 m away from the western edge of the bridge (Fig. 5.10 – Site 35). Indeed, the bridge appears to have been trying to hold back a massive slope failure which ended up pushing it off of the western abutment supports. The GEER team was not able to gain access to the eastern abutment and cannot comment on large-scale slope or localized abutment movements on that side which may have contributed to the failure.

Another spectacular roadway failure was caused by a massive landslide above Aratozawa Dam. The volume of the landslide was estimated to be 50 million cubic meters, of which approximately 1.5 million cubic meters slid into Aratozawa Reservoir. The landslide carried a section of road more than 3.5 km-long with it. Figure 5.11 (Site S27) shows aerial photographs of the reservoir before (left) and after (right) the earthquake. The red lines in the photographs highlight the section of road that extended from the reservoir up onto the mountain prior to the earthquake and subsequent landslide. As can be seen, much of the road was completely swept away and destroyed by the landslide. However, one set of switch-backs along the road remained relatively intact, despite being displaced approximately 300 m to the southeast. Figure 5.12 (Site

S72) shows pictures that were taken of the road along the southern-most extent of this section of switch-backs. Figure 5.13 (Site S73) shows pictures that were taken of the road along the northern-most extent of this section of switch-backs. Additional information about this landslide and the damage induced by the earthquake at Aratozawa Dam may be found in the report sections that address landslides and dams, respectively.

Other than the catastrophic bridge failure on Hwy 342 (refer to Fig's. 5.8 and 5.9), damage to bridges in the region was minor and predominantly characterized by seismic compression of approach fills (refer to Fig. 5.6) and permanent strain induced in some elastomeric bearings (Fig 5.14 – Site S1). Seismic compression of bridge approach fills was widespread with many bridges experiencing vertical displacements on the order of 20 – 30 cm between the superstructure and the embankment. A group of three bridges in close proximity to one another on Hwy 398 all experienced approach fill settlements of approximately 20 cm (Fig. 5. 15 – Site S54). Interestingly, the displacements on all three bridges were primarily observed on the uphill (northern) approach fills, while the downhill (southern) approach fills settled minimally. When approach fill displacements rendered vehicle passage difficult, they were typically remedied in the short term by constructing temporary ramps onto the bridge in one of the two lanes.

Figure 5.1: Landslide/rockfall debris covering Rt. 49 approximately 2 km south of the Iwate-Miyagi Prefecture border. The parent material and the blocked road can be seen in the top picture. A close-up view of the debris blocking the road can be seen in the bottom picture. The slide originated on the east-side of the road, ran down into a ravine and then upslope onto the road, indicating significant velocity. A small pond was actively building behind the failure. The slide was approximately 40-m high and 60-m wide and consisted primarily of rock with little soil (Site S16, N38.91498^{o} E140.9068^{o}, 6/26/08 16:30).

Figure 5.2: Landslide/rockfall debris covering Rt. 37 south of its intersection with Hwy 397. The parent material and the blocked road can be seen in the top picture. A close-up view of the debris blocking the road can be seen in the bottom picture. The slide originated on the north-side of the road and took out a rockfall barrier consisting of steel I-beams and chain-link fence. From a distance, the concrete gravity wall supporting the rockfall barrier did not appear to move. The slide was shallow, and approximately 15-m high by 50-m wide (Site S40, N39.0993^o E140.97252^o, 6/28/08 12:08).

Figure 5.3: Hwy 342 was swept away by a landslide (pictures taken from the south-east side of the failure). The top picture shows the abrupt end of the road with the remains of a tied-back earth retaining system in the background (concrete waler beams). The bottom picture shows a different view of the road failure from an offset angle. The tied-back wall above the former road indicates that this was a problematic slope before the earthquake. The slide was approximately 100-m wide at road level, and extended approximately 50-m above the road and 150-m below, to the bottom of the ravine (Site S31, N39.00532^o E140.84219^o, 6/28/08 9:45).

Figure 5.4: Embankment damage on Hwy 342 (pictures taken from the south-east side of the failure). The top picture shows minor settlement and extensional slumping of the embankment (~ 15 cm) in the foreground with another failure in the background indicated by the dipping rail and second set of cones. The bottom picture shows a close-up view of the second part of the embankment failure with vertical displacements ranging from 50 – 80 cm (Site S2, N38.97426° E140.9843°, 6/26/08 13:30).

Figure 5.5: Road embankment damage on Hwy 342 caused by lateral slumping to the south. The top picture is a view of the failure from the west, while the bottom picture is a view of the failure from the east. Long extensional cracks developed in both lanes of the roadway. The fissure that the SUV tipped over in is more than 1-m deep and 1-m wide (Site S34, N39.01288^{o} E140.86688^{o}, 6/28/08 10:15).

Figure 5.6: Settlement of a bridge approach fill on Hwy 342. The top picture is a view of the bridge from the south, showing the temporary ramp onto the bridge constructed in one lane. The bottom picture shows the expansion joint on the north side of the bridge which had opened up 6 cm out of its 8 cm of possible travel. The approach fill on the north-side of the bridge settled 23 cm, while the approach fill on the south-side settled 32 cm. The concrete bridge was approximately 80-m long and appeared to have no structural damage (Site S48, N39.03768^{o} E140.72435^{o}, 6/29/08 11:25).

Figure 5.7: Slope failure of an approximately 3-m high embankment on a country road south of Rt. 37. The failure was approximately 5-m wide at road level and slumped/rotated into the rice field below (Site S41, N39.09119^{o} E140.98671^{o}, 6/28/08 14:24).

Figure 5.8: Aerial view of the bridge collapse on Hwy 342. The picture was taken looking from south to north with the western abutment located on the left-hand side of the photo (Site S36, N39.0146^{o} E140.87862^{o}, 6/28/08 10:33).

Figure 5.9: Collapse of a two-span, steel girder bridge on Hwy 342. The top picture was taken from the western abutment and shows the western span in the foreground (which dropped approximately 3 m when it fell off of the western abutment supports) and the missing eastern span in the background (which was pulled off of the eastern abutment supports into the ravine as the bridge buckled over the center pier). The bottom picture was taken from the center pier and shows the eastern abutment and the collapsed eastern span of the bridge in the ravine below (Site S36, N39.0146^{o} E140.87862^{o}, 6/28/08 10:33).

Figure 5.10: Severe road distress on Hwy 342 leading up to the western abutment of the bridge collapse shown in Figure 5.8. The road was pulled apart in the form of extensional grabens over a distance of approximately 100 m leading up to the bridge. The grabens had vertical faces ranging from 2 – 3 m high (Site S35, N39.01449^o E140.87741^o, 6/28/08 10:23).

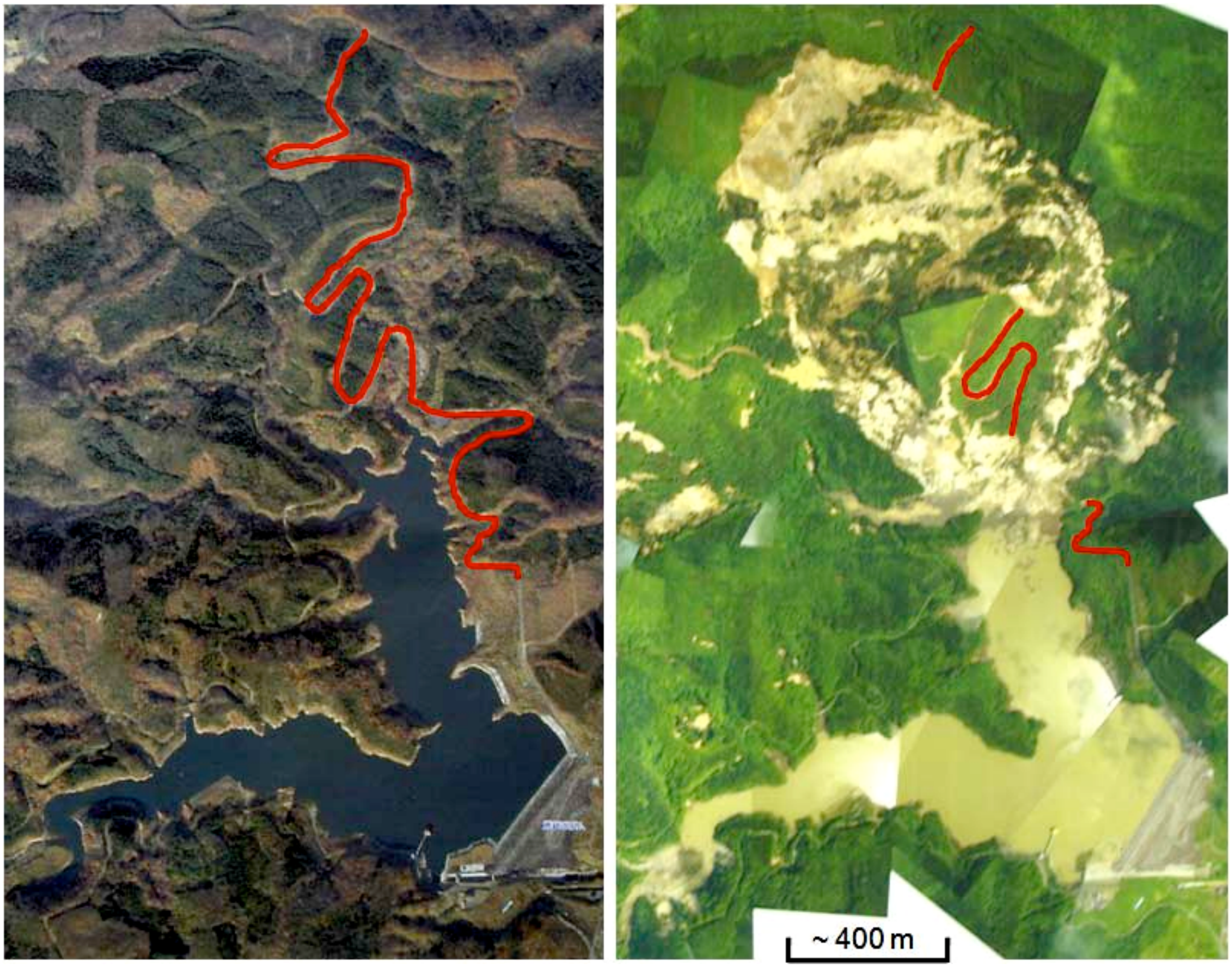

Figure 5.11: Aerial photographs of Aratozawa Dam before (left) and after (right) the earthquake. The massive landslide (estimated at 50 million cubic meters) seen in the post earthquake photo destroyed a section of road more than 3.5-km long. The section of the road affected by the land-slide is highlighted in red in both images. Notice the set of switch-backs in the post earthquake image that was left relatively intact despite being displaced approximately 300 m to the southeast by the landslide (Site S27, N38.8837^{o} E140.856^{o}, 6/27/08 17:00).

Figure 5.12: Photographs showing the condition of the road along the set of switch-backs that remained relatively intact after being displaced approximately 300 m to the southeast by the Aratozawa Dam landslide (the switch-back portion of the road can be seen in the center of the post earthquake photograph in Figure 5.10). The top photograph is a view looking due south from the southern-most tip of the intact switch-back section. The reservoir can be seen in the background. The bottom photograph was taken in the middle of the switch-back section (Site S72, N38.89557^{o} E140.8531^{o}, 6/30/08 16:30).

Figure 5.13: Photographs showing the condition of the road along the set of switch-backs that remained relatively intact after being displaced approximately 300 m to the southeast by the Aratozawa Dam landslide. The top photograph is a view looking due north from the northern-most tip of the intact switch-back section. Multiple large blocks within the landslide can be seen in the background. The bottom photograph was taken at the same location; however, it shows a view to the east along the travel path of the former roadway. The road at this point was displaced downward by approximately 50 m. Sections of the road can be seen in the background

(Site S73, N38.89832° E140.85341°, 6/30/08 16:17).

Figure 5.14: Nudo bridge on Hwy 342 (top photo) showed no signs of damage following the earthquake. However, the elastomeric bearings (bottom photo) on each side of the newer pedestrian foot bridge (blue handrails on the right-hand side of the top photo) showed permanent lateral offset of approximately 1 cm over the 10-cm bearing height. The older automobile bridge was not supported on elastomeric bearings and showed no signs of distress (Site S1, N38.96254° E141.00877°, 6/26/08 13:08).

Figure 5.15: Approach fill settlement (seismic compression) occurred on the uphill (northern) embankment on three bridges in close proximity to one another on Hwy 398. The vertical displacements ranged from 23 – 20 cm on each of the three uphill embankments yet were minimal on each of the three downhill (southern) approach fill embankments. Both of the photographs shown above were taken looking from north to south. The top photo shows settlement at one of the three bridges that required a temporary ramp to be constructed onto the bridge, while the bottom photo shows settlement of a similar magnitude on another bridge that was more spread out laterally and did not require a temporary ramp (Site S54, N38.98401^{o} E140.7041^{o}, 6/29/08 13:07).

Section 6 - Earth and Concrete Dams

The team was able to visit seven earth and concrete dams during the field reconnaissance. Deformations and damage to concrete dams was none, or minimal, although several instances of landslides entering reservoirs occurred and provide case histories of landslide induced seiches in reservoirs. On the other hand, several earthen dams suffered moderate deformations due to settlement of the crest. These provide excellent case histories of seismically-induced earth dam deformations. One large earthen dam, the Aratozawa Dam in Miyagi Prefecture, had a large landslide impact the reservoir sending water over the spillway. Nowhere in a central area did a dam fail. At one dam, the Isawa Dam in Iwate Prefecture, one worker was killed by rockfall at the dam abutment. Landslide impacts to reservoir waters and moderate deformations of earth dams provide some of the most important geo-engineering case histories for the Iwate-Miyagi Nairiku earthquake.

Aratozawa Earth Dam

The most significant case history of earth dam deformation occurred at the Aratozawa (Indigo Dye Lake) Dam in Miyagi Prefecture (Site 27; N38.8837°, E140.856°). Aratozawa Dam is a large earth dam that was slightly damaged during the earthquake. It is of interest for several reasons: (1) It is the largest earth dam in close proximity to the earthquake epicenter, (2) a massive landslide above the dam partially slid into the reservoir and created a large wave that overtopped the spillway, (3) a 3-level downhole ground motion array recorded the earthquake motions at the dam, and (4) some minor cracking, and settlements ranging from 20 – 40 cm, were observed along the crest of the dam following the earthquake.

During the earthquake, the reservoir behind the dam was impacted by a large landslide of approximately 50,000,000 cubic meters. Some portion of that landslide estimated to be approximately 1,500,000 cubic meters, slid about 500 m into the reservoir sending a large seiche across and over the spillway to the valley below. No water crossed the crest of the reservoir. This provides an excellent case history of a landslide of large size entering a lake at high velocity.

Aratozawa Dam is an earth dam that is approximately 75-m high, 346-m wide at the base, and 10-m wide at the crest. The upstream slope of the dam is 2.7 horizontal to 1.0 vertical and the downstream slope is 2.1 horizontal to 1.0 vertical. The crest is approximately 400-m long. The dam is composed of a ??? core and a ??? shell … It is also instrumented with a 3-level downhole array of ??? accelerometers that recorded the earthquake ground motions. These accelerometers are located in three adjacent boreholes at the mid-point of the crest, and are fixed at depths of ???, ???, and ??? below the surface.

The clay core of the Aratozawa dam settled along the axis of the dam up to 400 mm and the Rock fill shells on either side settled between 179 mm to 198 mm, approximately half the settlement of the core. The upstream shell deformed laterally towards the reservoir between 24 and 43 mm. The dam also moved permanently, horizontally to the north approximately along the axis of the crest of the dam between 11 and 60 mm. Despite the deformations, there was no apparent damage to the facing on the downstream or upstream sides of the reservoir. Prior to the earthquake, the crest road between the two abutments climbed linearly to the center of the dam. Post-earthquake settlements are observable on the north and south ends of the dam crest resulting in an undulating, irregular and depressed surface. Surface cracks were observed on the southern end of the dam where the concrete spillway meets a soil abutment. At the time of the earthquake, the reservoir was full nearly to the tree line. It is now being drawn down approximately 50 cm per day and will be empty by September to fully inspect the dam and the impact of the landslide on the north arm of the reservoir.

The effect of the differential settlements of the rockfill shell and core were to depress the crest and cause rotation of monuments inward toward the center line of the dam. The crest road is a bordered by granite columns that are held in place at their base by a small rebar peg and connected to one another by a chain. Several of these monuments collapsed in irregular directions. The remaining standing monuments on both the upstream and downstream side were inclined toward the center of the crest due to the settlement of the core. These monuments were vertical prior to the earthquake. Another indication of core settlement is an observation pipe that emerged from a manhole near the center of the dam crest. This pipe is for estimating normal (static) crest and internal settlements of the dam. At the time of the GEER observation, the pipe appears to have moved upwards relative to the dam crest approximately 27 cm. We believe that the pipe may be partially dragged down with the dynamically settling crest approximately 13 cm and otherwise decoupled from the remaining settlement of the crest. This allowed it to emerge from a manhole cover. The sensor hole and pipe used to monitor settlement is in 5 m segments and extends 75 m to the bottom of the dam. A tunnel beneath the core of the dam was dry prior to the earthquake and is now leaking at approximately 1 liter per minute, indicating possible minor cracking of the core.

Figure 6.1 Aerial photo of the Aratozawa dam and reservoir prior to the earthquake. Image courtey of the Aratozawa dam operators, Miyagi Prefecture.

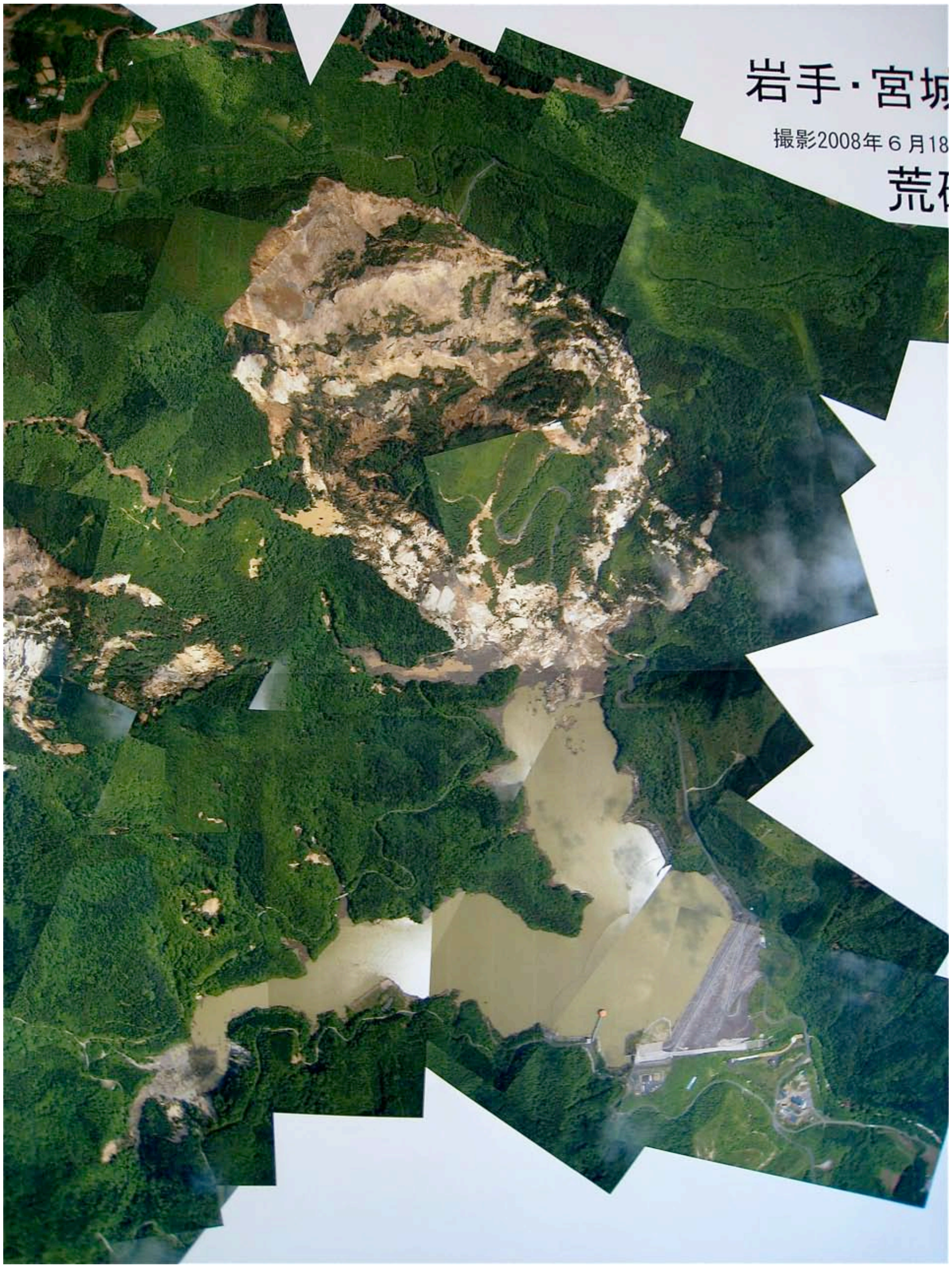

Figure 6.2 Aerial photo collage of the Aratozawa dam and reservoir on June 18, 2008, four days after the earthquake. Image courtey of the Aratozawa dam operators, Miyagi Prefecture.

Figure 6.3 Spillway on the south end of Aratozawa dam. The seiche from the landslide entering the reservoir on the north arm sent water over the top of the spillway on the right, and down the concrete water line.

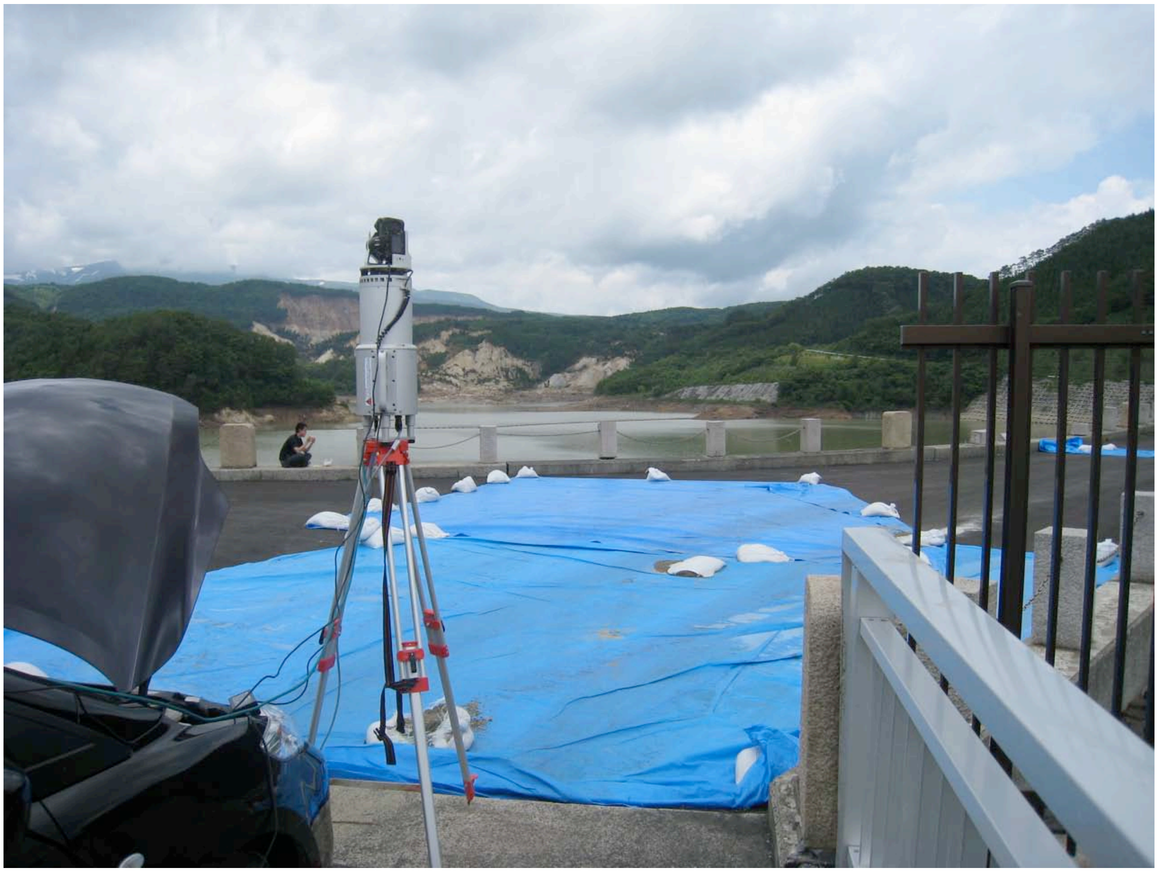

Figure 6.4 Blue tarps on the south end of the crest of the Aratozawa dam adjacent to the spillway. The tarps cover cracks in the pavement. Soil settled along the crest at the edge of the spillway resulting in a step at edge of the concrete and tarp.

Figure 6.5 Lidar scanner on the northern end of the dam crest, looking east toward the downstream side of the dam. Granite monuments line the roadway of the dam crest and are anchored by a rebar peg. Along the crest, several monuments pulled free of the pegs and collapsed in random directions.

At the Aratozawa Dam we gathered LiDAR data in 13 scans along the crest of the dam and from vantage points allowed us to image the up and down stream shells.

Isawa Earth Dam

The reconnaissance team visited the visitor center of the Isawa Dam in Iwate Prefecture (Site 38; N39.11977°, E140.93497°). this is a new earth dam under construction to enlarge the reservoir capacity of a smaller up-river dam. This dam site was affected by numerous landslides and rockfall. One rockfall killed a worker applying shotcreate at an abutment. The reconnaissance team was not able to access the crest of the either the new or old dam and have no measurements of deformations. Workers at the visitor center informed the team that there were minor deformations. At the new dam construction site, ongoing daily construction had already covered any observable deformations.

Masazawa Earth Dam.

The Masazawa earth dam in Iwate Prefecture is located at site 42 of the reconnaissance (N39.100905°, E140.966859°). This small dam is approximately 35 m high. It is 9 m wide at the crest and 222m wide at the base. This site was our first LIDAR data collection location. This earth dam experienced significant deformation of up to 1.5 meters vertical settlement on the upstream side of the crest. The dam also experienced wall movement of the western upstream shell. Based on vegetation growing low on the reservoir slopes, water appears to have been low at the time of the earthquake and no water crossed the spillway or crest of the dam. Along the crest of the dam, transverse cracks were noted in the pavement. Blue tarps also covered portions of the downstream slope of earthen embankment. Settlement between spillway and embankment were between 10 and 20 cm and irregular. The upstream edge of the crest, and curb of the crest Road was severely tilted towards the lake. Six LiDAR scans were taken to capture the deformations of this dam. Reflectors for the LIDAR data collection were placed arbitrarily on the guard rails and fence perimeter of the dam. These reflectors are used to establish a project coordinate system for the LiDAR data set.

Figure 6.6 Downstream face of Masawa dam, Iwate Prefecture, site 42. Blue tarps cover embankment cracks below the dam crest. The Lidar scanner is imaging the east face of the dam.

Figure 6.7 Damaged crest of Masazawa dam, the reservoir side is on the west (right). The upstream side of the crest road slid downslope carrying the curb and guard rail.

Figure 6.8 The failed upstream side of Masazawa dam crest covered by blue tarps.

Koda Earth Dam

The Koda Dam, located in northwestern Miyagi Prefecture at Site 59 (N38.75556°, E140.8421°) is a small 35 m tall clay core dam with earth and rockfill shells. The upstream slope of the dam is 2.8-1 and the downstream slope is 2.0-1.   The clay core is 9 meters wide at the crest and broadens to a 43 m stepped cap that blankets the foundation rock. There was minor apparent damage to earth dam crest with maximum settlements of 10 cm and some compression of curb stones along the crest. Blue tarps covered portions of the crests that were undergoing repair work for pavement cracking.

Hara-Cho Earth Dam

Hara-Cho earth dam is located in Northwestern Miyagi Prefecture near the border of Yamagata Prefecture at site 56 (38.79749, 140.63966). This small dam has a crest width of 8 m and a broad berm protecting the downslope side of the dam. The dam is earthen but has no densified clay-core. This dam has a concrete cutoff wall and core.   The Hara-Cho Dam had crest cracks of approximately 1 cm and some indications of compression of curbstone resulting in spalling. Cracking was minor and covered by blue tarps.

Kurikama Concrete Dam

The Kurikama Concrete Dam is located in northwestern Miyagi Prefecture at site 66 (N38.9064°, E140.918°). There was no damage to this dam, however a large landslide entered the reservoir at the north side of the dam. The reservoir water seiched but did not cross the spillway. Several large landslides on the west end of the reservoir raised concern about other landslides entering the waters, and the reservoir is being emptied as a precaution.

Figure 6.9 The undamaged spillway of the concrete Kurikama dam, Miyagi Prefecture. Water was being released from the reservoir to drain it for inspection.

Figure 6.10 The undamaged crest of the concrete Kurikama dam, Miyagi Prefecture.

Figure 6.11 A landslide entered the reservoir of Kurikama dam, approximately 150 meters north of the dam.

Naruko Concrete Dam

Naruko Concrete Dam is located in northwestern Miyagi Prefecture at Site 57 (N38.75377, E140.70644) and had no apparent damage. This dam was not impacted by landslides.

Figure 6.12 The undamaged Naruko dam, Miyagi Prefecture. No landslides were observed on the margins of this dam.

Hanayama Concrete Dam

The Hanayama Dam is located at Site 60 in northwestern Miyagi Prefecture near the border of a Iwate prefecture (N38.78021°, E140.86836°). This dam is a large concrete structure with no apparent damage. Some minor concrete cracking was observed at the control-building perimeter and asphalt, with cracks 1-2 cm in width. A landslide entered into the reservoir water and apparently elevated water levels.

Section 7 – Observations from Advanced Reconnaissance Tools

SASW

The nonintrusive Spectral Analysis of Surface Waves (SASW) method was used to obtain three shallow shear wave velocity (V_s) profiles across the crest of Aratozawa Dam (additional information about Aratozawa Dam may be found in Section 6). Shear wave velocity measurements at this site were desired for several reasons: (1) to potentially delineate the depth and thickness of soft layers near the crest of the dam that may have contributed to the observed crest settlement through seismic compression, and (2) to aid in future dynamic analyses using the recorded downhole array ground motions at the dam.

The SASW field measurements were made using three 4.5 Hz geophones, a 'pocket-portable' dynamic signal analyzer, and two hammers purchased in Japan (Fig. 7.1 – Site 27). The geophones are model GSC-11D's manufactured by Geo Space Technologies, while the analyzer is a 'pocket portable' Quattro system manufactured by Data Physics Corporation. The Quattro is a USB powered, 4-input channel, 2-output channel dynamic signal analyzer with 205 kHz simultaneous sampling rate, 24 bit ADC, 110 dB dynamic range, and 100 dB anti-alias filters. It is controlled with a flexible, windows-based software package (Data Physics Signal Calc) that has measurement capabilities in both the time and frequency domain. The compact, highly portable nature of this setup is ideal for earthquake reconnaissance efforts where shallow V_s profiles may be desired.

SASW data was collected at three separate locations along the approximately 400-m long crest of the dam. These three locations were simply designated as SASW 1, SASW 2 and SASW 3. The latitude and longitude coordinates for the centerline of each SASW array are provided in Table 7.1. SASW 1 is located at the south-western end of the crest near the spillway, SASW 2 is located near the center of the crest (in close proximity to the downhole array boreholes), and SASW 3 is located at the north-eastern end of the crest. At all three locations, receiver spacings of 0.5, 1, 2, 4 and 8 m were used to collect surface wave data. The tests took less than 30 minutes per location.

The experimental dispersion curve data obtained at Site 1 are provided in Fig. 7.2, both in terms of wavelength and frequency. At this site, experimental wavelengths between approximately 0.2 - 14 m were resolved at frequencies between approximately 20 – 1000 Hz. The theoretical dispersion curve that was fit to the experimental data is also shown in Fig. 7.2. The theoretical dispersion curve was obtained through iterative forward modeling using the '3D solution' in WinSASW (Joh 1996), which accounts for fundamental and higher-mode surfaces waves as well as reflected body waves. The dispersion trend shows a velocity inversion at short wavelengths (high frequencies) followed by a normally dispersive trend of increasing phase velocity with increasing wavelength (decreasing frequency). The velocity inversion is caused by a stiff asphalt layer at the ground surface, which is underlain by relatively soft compacted fill.

The V_s profile corresponding to the final theoretical dispersion curve for Site 1 is shown in Fig. 7.3. The properties assumed for each layer in the profile through forward modeling are provided in Table 7.2. The maximum depth of the V_s profile was limited to approximately ½ of the maximum measured wavelength. It can be seen that the fill is quite soft (less than approximately 200 m/s) down to a depth just less than 2 m. In particular, a very soft layer (just over 100 m/s) more than 20 cm thick exists just below the asphalt. These soft layers likely played a role in the crest settlement observed at the dam. It should be noted that soil liquefaction in these shallow layers did not occur as the water level in the reservoir at the time of the earthquake was well below the crest.

The dispersion curve data for sites SASW 2 and SASW 3 are similar to that shown for SASW 1, and are therefore not shown for the sake of brevity. However, all three V_s profiles are compared in Fig. 7.4. It can be seen that the Vs profiles for all three sites are quite similar, and primarily differ only in the depth to where the velocity surpasses 400 m/s. The depth to this stiffer layer is greatest near the center of the crest (SASW 2) and is smaller near the abutments (SASW 1 and 3). These results seem to agree with field observations that the crest was visibly higher at the center line of the dam than at the abutments (i.e. a thicker layer of soft surficial fill exists near the center of the crest). Furthermore, each velocity profile shows a very soft layer (~ 100 m/s) directly below the asphalt pavement. The assumed properties for each layer in the profiles for sites SASW 2 and SASW 3 are provided in Tables 7.3 and 7.4, respectively.

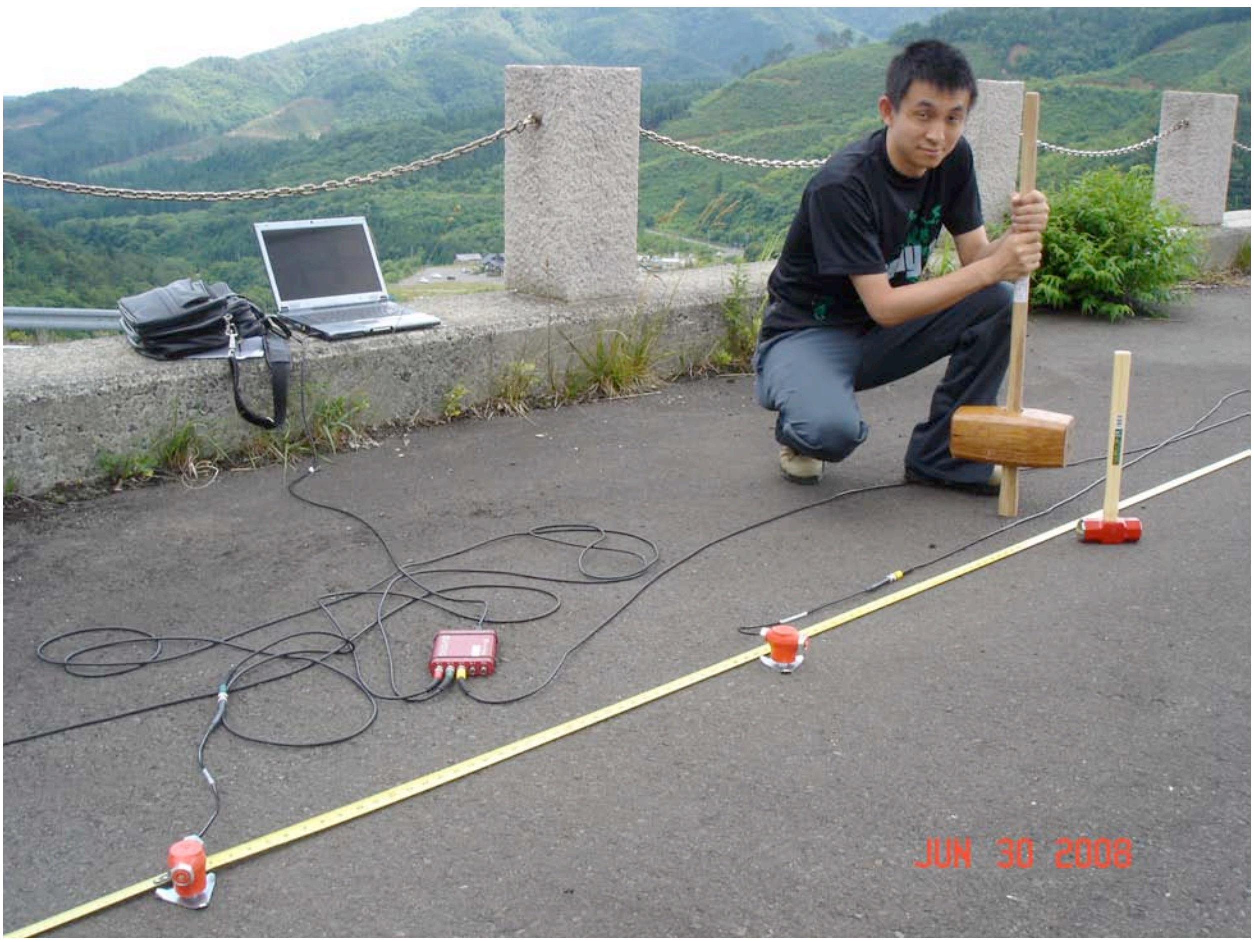

Figure 7.1: Compact, highly portable equipment owned by the University of Arkansas was used to conduct shallow SASW tests at three locations along the crest of Aratozawa Dam. The field measurements were made using three 4.5 Hz geophones, a 'pocket-portable' dynamic signal analyzer, and two hammers purchased in Japan. The V_s profiles generated from these measurements extended to a depth of approximately 7 m. The field measurements took less than 30 minutes per location (Site S27, N38.8837°

E140.856°, 6/27/08 17:00).

Table 7.1: Decimal degree latitude and longitude coordinates for the three locations where SASW tests were performed along the crest of Aratozawa Dam

Location	Latitude	Longitude
SASW 1	38.884657	140.856332
SASW 2	38.885744	140.857280
SASW 3	38.887219	140.858417

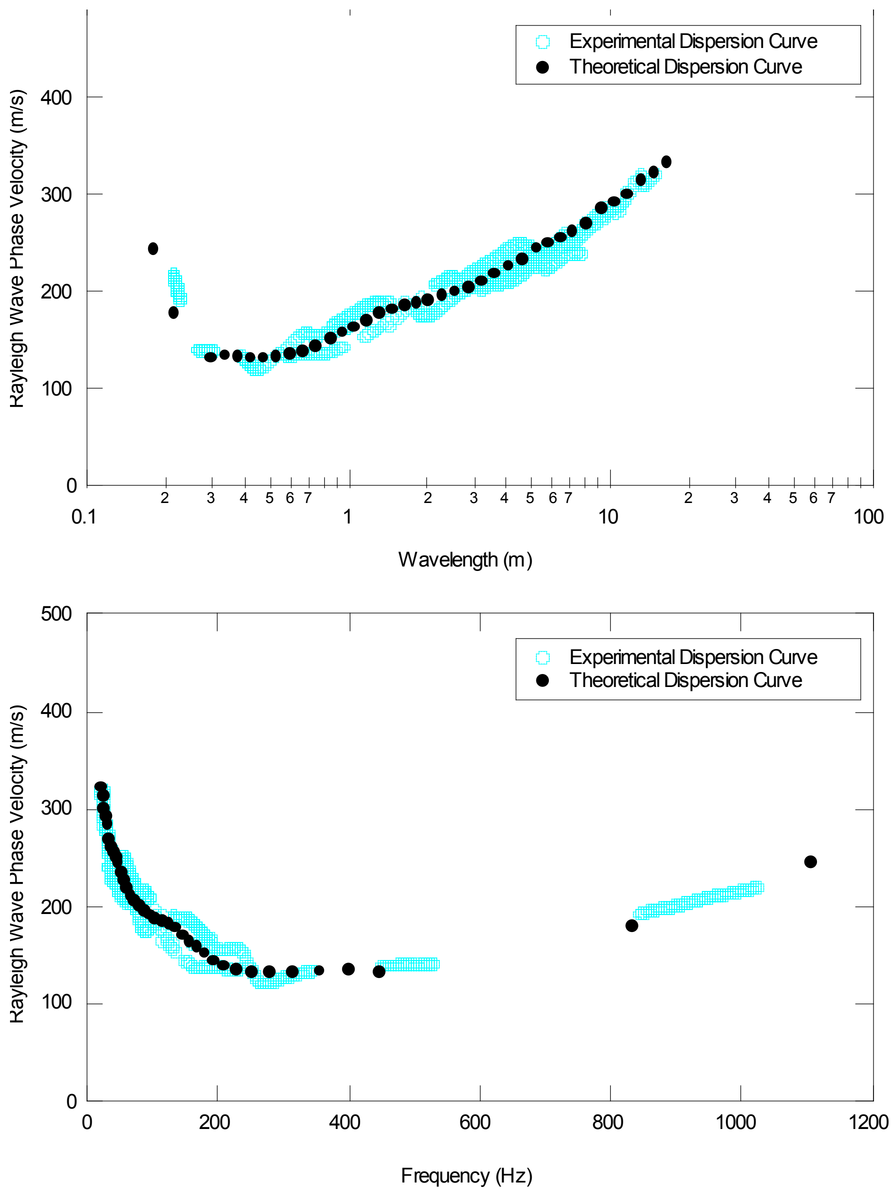

Figure 7.2: Experimental and theoretical dispersion curves for location SASW 1 on the crest of Arato-zawa Dam.

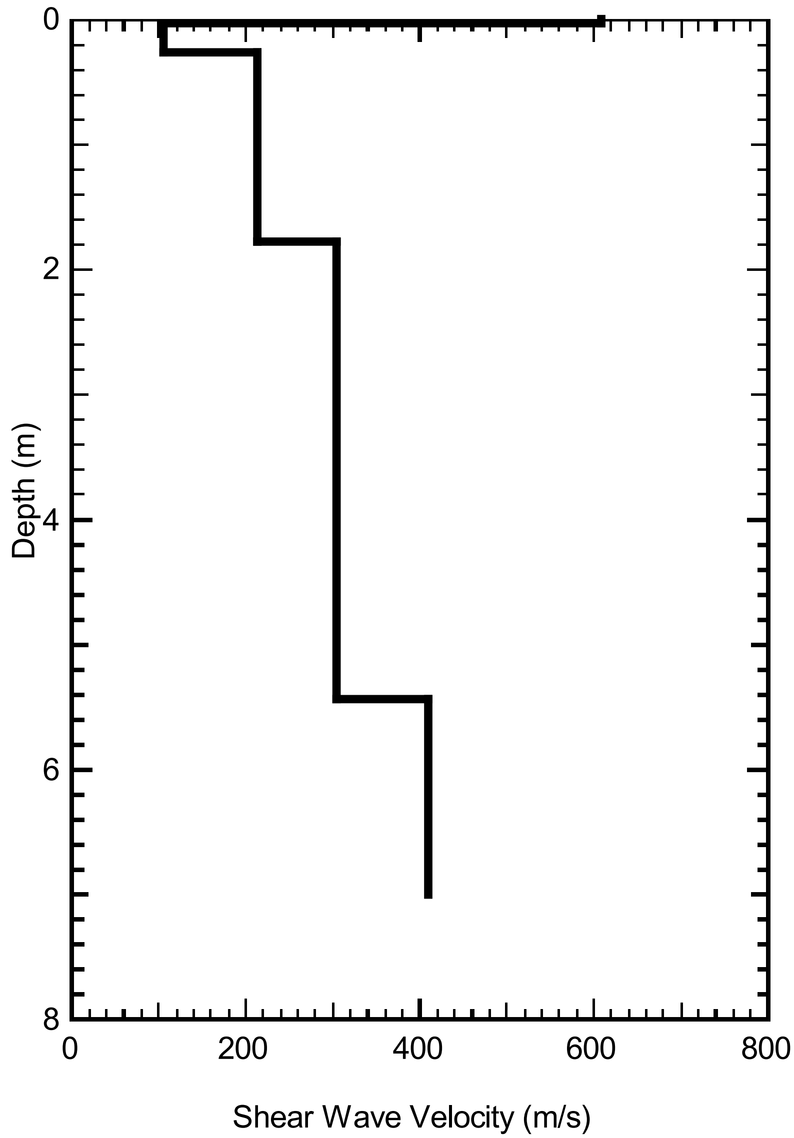

Figure 7.3: Shear wave velocity profile for location SASW 1 on the crest of Aratozawa Dam.

Table 7.2: Final properties assumed for each layer in the profile through forward modeling of location SASW 1 on the crest of Aratozawa Dam

Layer number	Depth to top of layer (m)	Layer thickness (m)	P-wave velocity (m/s)	Shear wave velocity (m/s)	Poisson's ratio	Unit weight (kN/m^3)
1	0	0.03	1141	610	0.3	22.0
2	0.03	0.23	200	107	0.3	20.4
3	0.26	1.52	399	213	0.3	20.4
4	1.78	3.66	570	305	0.3	20.4
5	5.44	1.56	770	411	0.3	20.4

*Depth of profile limited to the maximum wavelength measured divided by two (i.e. $\lambda_{max}/2$)

Table 7.3: Final properties assumed for each layer in the profile through forward modeling of location SASW 2 on the crest of Aratozawa Dam

Layer number	Depth to top of layer (m)	Layer thickness (m)	P-wave velocity (m/s)	Shear wave velocity (m/s)	Poisson's ratio	Unit weight (kN/m^3)
1	0	0.03	1141	610	0.3	22.0
2	0.03	0.17	200	107	0.3	20.4
3	0.20	1.22	371	198	0.3	20.4
4	1.42	4.57	570	305	0.3	20.4
5	5.99	1.00	770	411	0.3	20.4

*Depth of profile limited to the maximum wavelength measured divided by two (i.e. $\lambda_{max}/2$)

Table 7.4: Final properties assumed for each layer in the profile through forward modeling of location SASW 3 on the crest of Aratozawa Dam

Layer number	Depth to top of layer (m)	Layer thickness (m)	P-wave velocity (m/s)	Shear wave velocity (m/s)	Poisson's ratio	Unit weight (kN/m^3)
1	0	0.05	1141	610	0.3	22.0
2	0.05	0.23	200	107	0.3	20.4
3	0.27	1.22	399	213	0.3	20.4
4	1.49	3.05	570	305	0.3	20.4
5	4.54	2.46	798	427	0.3	20.4

*Depth of profile limited to the maximum wavelength measured divided by two (i.ę.$\lambda_{max}/2$)

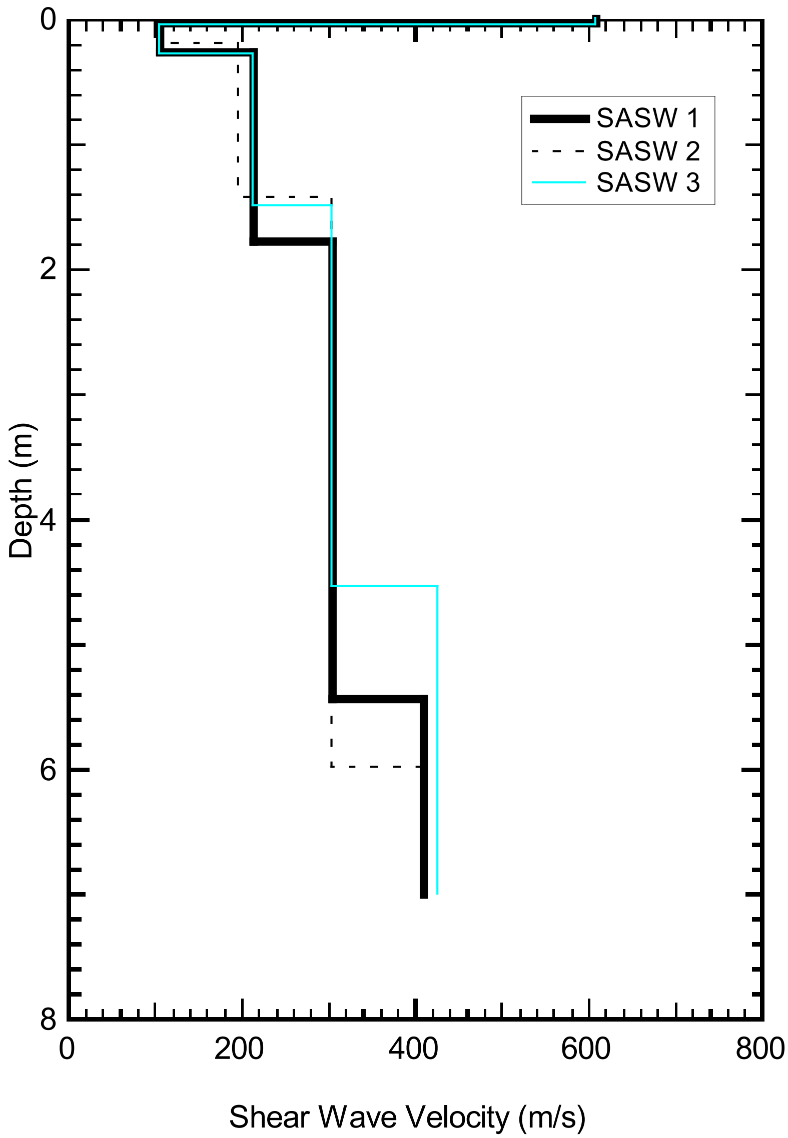

Figure 7.4: Comparison of shear wave velocity profiles for locations SASW 1, SASW 2 and SASW 3 on the crest of Aratozawa Dam.